NAVAL POSTGRADUATE SCHOOL

MONTEREY, CALIFORNIA

THESIS

OPTIMIZING GAS GENERATOR EFFICIENCY IN A FORWARD OPERATING BASE USING AN ENERGY MANAGEMENT SYSTEM

by

Ryan L. Kelly

June 2013

Thesis Co-Advisors: Giovanna Oriti
Alexander L. Julian

Approved for public release; distribution is unlimited

THIS PAGE INTENTIONALLY LEFT BLANK

REPORT DOCUMENTATION PAGE			*Form Approved OMB No. 0704–0188*
Public reporting burden for this collection of information is estimated to average 1 hour per response, including the time for reviewing instruction, searching existing data sources, gathering and maintaining the data needed, and completing and reviewing the collection of information. Send comments regarding this burden estimate or any other aspect of this collection of information, including suggestions for reducing this burden, to Washington headquarters Services, Directorate for Information Operations and Reports, 1215 Jefferson Davis Highway, Suite 1204, Arlington, VA 22202–4302, and to the Office of Management and Budget, Paperwork Reduction Project (0704–0188) Washington DC 20503.			
1. AGENCY USE ONLY ***(Leave blank)***	**2. REPORT DATE** June 2013	**3. REPORT TYPE AND DATES COVERED** Master's Thesis	
4. TITLE AND SUBTITLE OPTIMIZING GAS GENERATOR EFFICIENCY IN A FORWARD OPERATING BASE USING AN ENERGY MANAGEMENT SYSTEM		**5. FUNDING NUMBERS** **N/A**	
6. AUTHOR(S) Ryan L. Kelly			
7. PERFORMING ORGANIZATION NAME(S) AND ADDRESS(ES) Naval Postgraduate School Monterey, CA 93943–5000		**8. PERFORMING ORGANIZATION REPORT NUMBER**	
9. SPONSORING /MONITORING AGENCY NAME(S) AND ADDRESS(ES) N/A		**10. SPONSORING/MONITORING AGENCY REPORT NUMBER**	
11. SUPPLEMENTARY NOTES The views expressed in this thesis are those of the author and do not reflect the official policy or position of the Department of Defense or the U.S. government. IRB Protocol number ____N/A____.			
12a. DISTRIBUTION / AVAILABILITY STATEMENT Approved for public release; distribution is unlimited		**12b. DISTRIBUTION CODE** A	

13. ABSTRACT (maximum 200 words)

A Forward Operating Base (FOB) is designed to support combat operations in an austere environment, which often lacks pre-existing infrastructure. On-site diesel generators are the primary source of FOB electricity. Traditionally, each generator is connected to its own set of loads and operates independently from other generators. The benefits of transitioning from traditional generator employment to an alternative architecture using an Energy Management System (EMS) were investigated in this thesis. The EMS provides an interface between power sources, loads, and energy storage elements to form a microgrid. Using power electronics and programmable logic, the EMS provides capabilities such as power source selection, power metering, flow control, and peak power management. These capabilities enable more efficient generator utilization by matching real time load demand to the smallest capable power source, reducing overall fuel consumption. The EMS offers redundancy as it can connect any one of multiple power sources to critical loads. A hardware-based laboratory experiment demonstrated the ability to transition from one power source to another while providing uninterrupted current to the load. The results of the experiment validate a Simulink model of the EMS. An example load profile was applied to the model to compare overall fuel consumption between the traditional architecture and EMS-enabled microgrid.

14. SUBJECT TERMS Energy management system, forward operating base (FOB), generators, Microgrid, power electronics			**15. NUMBER OF PAGES** 99
			16. PRICE CODE
17. SECURITY CLASSIFICATION OF REPORT Unclassified	**18. SECURITY CLASSIFICATION OF THIS PAGE** Unclassified	**19. SECURITY CLASSIFICATION OF ABSTRACT** Unclassified	**20. LIMITATION OF ABSTRACT** UU

NSN 7540–01–280–5500

Standard Form 298 (Rev. 2–89)
Prescribed by ANSI Std. 239–18

THIS PAGE INTENTIONALLY LEFT BLANK

Approved for public release; distribution is unlimited

OPTIMIZING GAS GENERATOR EFFICIENCY IN A FORWARD OPERATING BASE USING AN ENERGY MANAGEMENT SYSTEM

Ryan L. Kelly
Captain, United States Marine Corps
B.S., United States Naval Academy, 2004

Submitted in partial fulfillment of the
requirements for the degree of

MASTER OF SCIENCE IN ELECTRICAL ENGINEERING

from the

NAVAL POSTGRADUATE SCHOOL
June 2013

Author: Ryan L. Kelly

Approved by: Giovanna Oriti
Thesis Co-Advisor

Alexander L. Julian
Thesis Co-Advisor

R. Clark Robertson
Chair, Department of Electrical and Computer Engineering

THIS PAGE INTENTIONALLY LEFT BLANK

ABSTRACT

A Forward Operating Base (FOB) is designed to support combat operations in an austere environment, which often lacks pre-existing infrastructure. On-site diesel generators are the primary source of FOB electricity. Traditionally, each generator is connected to its own set of loads and operates independently from other generators. The benefits of transitioning from traditional generator employment to an alternative architecture using an Energy Management System (EMS) were investigated in this thesis. The EMS provides an interface between power sources, loads, and energy storage elements to form a microgrid. Using power electronics and programmable logic, the EMS provides capabilities such as power source selection, power metering, flow control, and peak power management. These capabilities enable more efficient generator utilization by matching real time load demand to the smallest capable power source, reducing overall fuel consumption. The EMS offers redundancy as it can connect any one of multiple power sources to critical loads. A hardware-based laboratory experiment demonstrated the ability to transition from one power source to another while providing uninterrupted current to the load. The results of the experiment validate a Simulink model of the EMS. An example load profile was applied to the model to compare overall fuel consumption between the traditional architecture and EMS-enabled microgrid.

THIS PAGE INTENTIONALLY LEFT BLANK

TABLE OF CONTENTS

THIS PAGE INTENTIONALLY LEFT BLANK

LIST OF FIGURES

LIST OF TABLES

THIS PAGE INTENTIONALLY LEFT BLANK

LIST OF ACRONYMS AND ABBREVIATIONS

A/D	Analog-to-Digital
AC	Alternating Current
Ah	Amp-hours
COC	Combat Operations Center
DoD	Department of Defense
ECU	Environmental Control Unit
EMS	Energy Management System
FOB	Forward Operating Base
FPGA	Field Programmable Gate Array
GBOSS	Ground Based Operational Surveillance System
IGBT IPM	Insulated Gate Bipolar Transistor Integrated Power Module
LCD	Liquid Crystal Display
LED	Light-emitting Diode
PC	Personal Computer
PCB	Printed Circuit Board
RC	Resistor-capacitor
RMS	Root-mean-square
SoC	State of Charge
TQG	Tactical Quiet Generator
TTL	Transistor-transistor Logic
USB	Universal Serial Bus
USMC	United States Marine Corps

THIS PAGE INTENTIONALLY LEFT BLANK

EXECUTIVE SUMMARY

A Marine Corps Forward Operating Base (FOB) is a self-contained military base designed to support combat operations in an austere environment, often without pre-existing infrastructure. Similar in function to a permanent military base, a FOB contains planning spaces, billeting tents, and a variety of equipment, which all require electricity. Lacking a utility grid, the primary source of a FOB's electrical power is provided on-site by diesel generators.

Marines and soldiers are responsible for the transportation, safe employment, maintenance, and re-fueling of forward-deployed generators. These efforts enable sustained generator operation but also impose significant logistical challenges to deployed forces. For instance, the cost of fuel alone is a tremendous financial burden to the Department of Defense (DoD) at an estimated $400 per gallon delivered to a FOB [1]. In addition to the high dollar cost of fuel, the necessity of resupply convoys to deliver the fuel pose significant risk to U.S. armed forces. Former Commandant of the Marine Corps, General James Conway, related that 10–15 percent of Marine casualties occur during fuel and water convoy operations alone [2]. More efficient generator use presents opportunity to reduce a FOB's overall fuel consumption and, in turn, save money while reducing risk to American troops.

The efficiency of a diesel generator is related to its electrical power output, as shown in Figure 1 for an example 10 kW tactical quiet generator (TQG). The objective of this thesis is to introduce an Energy Management System (EMS) into the FOB power system in order to more efficiently utilize generators and reduce overall fuel consumption. For a given load a smaller generator at a high operating point is more efficient than a large generator at a low operating point in terms of fuel cost per unit of power. The EMS enables increased efficiency by ensuring that the smallest generator is selected to power the load; furthermore, if the batteries are charged and sufficiently rated, the EMS can shut down both generators and draw power from batteries alone.

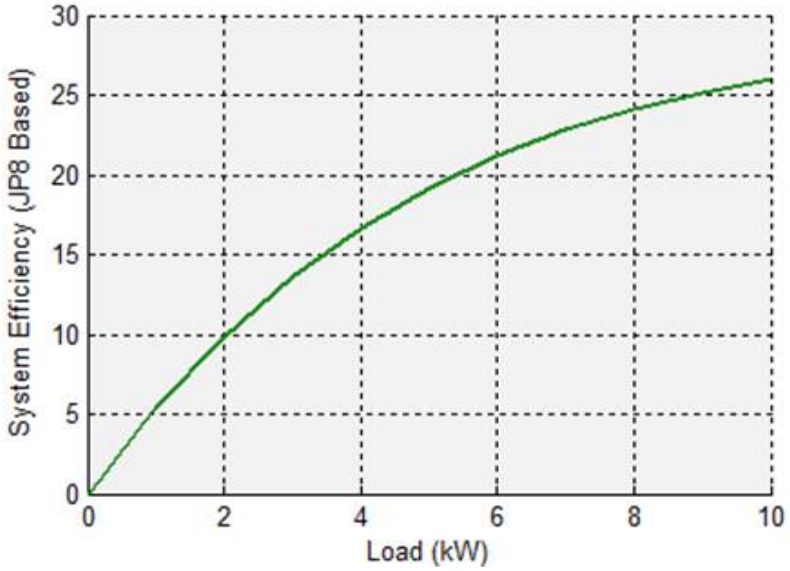

Figure 1. Efficiency of a 10 kW generator versus load. After [3].

The EMS provides an interface between loads, power sources, and energy storage elements and is depicted in Figure 2. The blue box in Figure 2 highlights the EMS's battery pack, boost converter, and H-bridge inverter, which allow the EMS to inject current to power a load or draw current to charge the battery pack. Logic stored on a field programmable gate array (FPGA) dictates which power source the EMS selects based upon the load's power demand. Depending upon the load demand, the EMS can connect to an external voltage source or operate off of batteries alone. A handoff from one voltage source to another is depicted in Figure 2 in two steps. In step 1 the EMS disconnects from Source A by opening a switch. Once disconnected from Source A, the EMS then connects to Source B as shown by Step 2.

A laboratory experiment was conducted to demonstrate the EMS's ability to disconnect from an external voltage source, operate using batteries alone and then reconnect to an external voltage source while maintaining uninterrupted current to the load. The voltages and currents produced when disconnecting the EMS from Source A are shown in Figure 3, and the corresponding waveforms for the connection to Source B are shown in Figure 4.

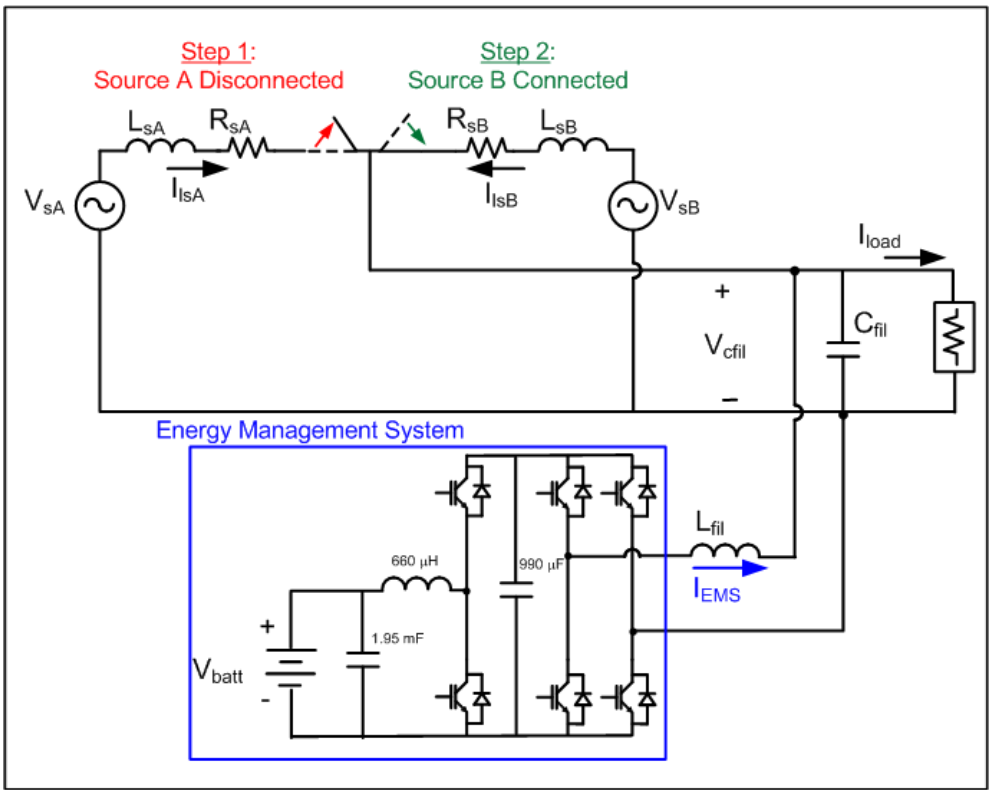

Figure 2. Microgrid formed by the EMS, battery bank, two external voltage sources, and a resistive load.

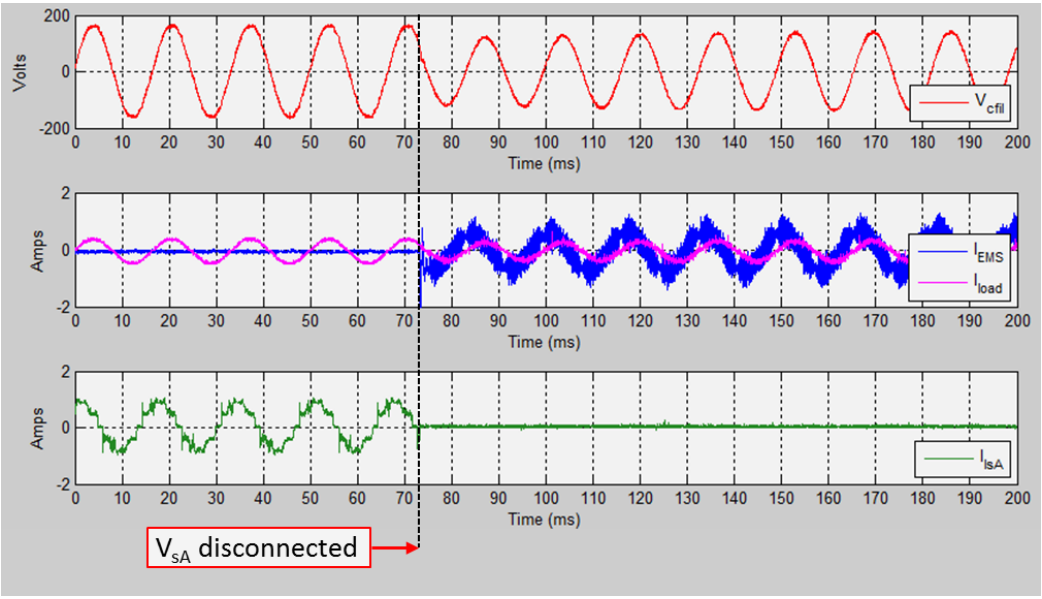

Figure 3. EMS provides power to the load after it disconnects V_{sA}. (V_{cfil} is the AC bus servicing the loads).

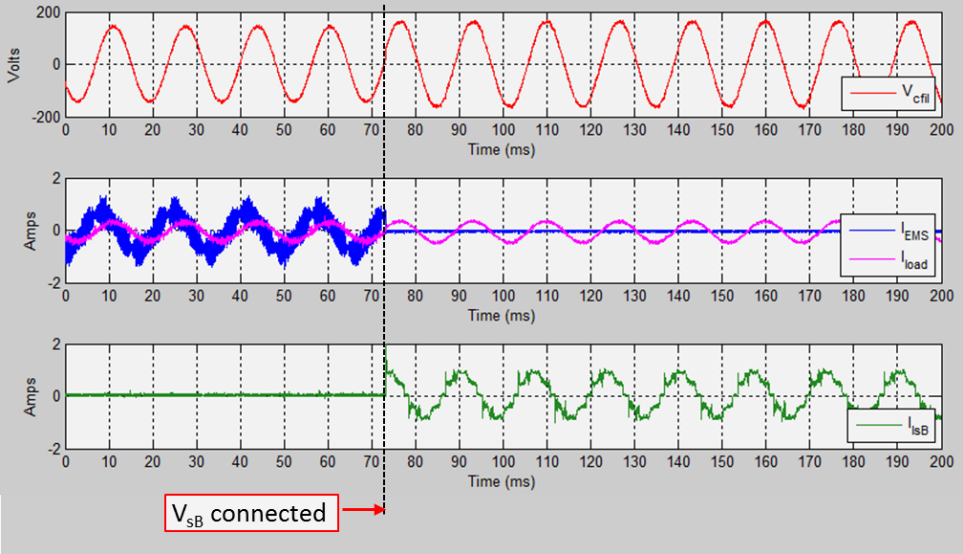

Figure 4. EMS stops providing power to the load after it connects to V_{sB}.

A traditional method of generator employment is commonly used in FOBs where each generator is directly connected to its own set of loads [4]. An example of traditional two-generator employment is shown in the top pane of Figure 5. A notional profile representing each of the two generator's load demand, as well as their sum, is depicted over a 24-hour period in the bottom pane of Figure 5. In this scenario the critical loads are connected to the 5 kW generator, and the non-critical loads are connected to the 20 kW generator. Critical loads are those electrical devices that must be powered at all times to ensure safety or mission success. Non-critical loads may be briefly turned off without causing a major disruption to safety or operational requirements. While it is not necessary that under traditional generator employment the critical loads be connected to one generator and non-critical loads to the other, examples of such configurations do indeed exist [4], and it is convenient for comparison later to move forward with this configuration.

Annotated boxes surrounding portions of the load profile in Figure 5 contain information regarding a generator's loading. By visual inspection it is clear that both the 5 kW and 20 kW generators run at less than 50 percent of their rated maximum load

throughout the notional scenario. Since a generator's efficiency is directly proportional to its loading, such low generator loading as presented in Figure 5 gives room for optimization.

Generator loading, fuel flow data, and fuel consumed by each generator under the traditional method of employment is contained in Table 1. Fuel flows were estimated using each generator's capacity, operating point, and data from [5] and [6]. Using the traditional method of generator employment shown in Figure 5, we see that the two generators consumed a total of 22.7 gallons of fuel in a 24-hour period.

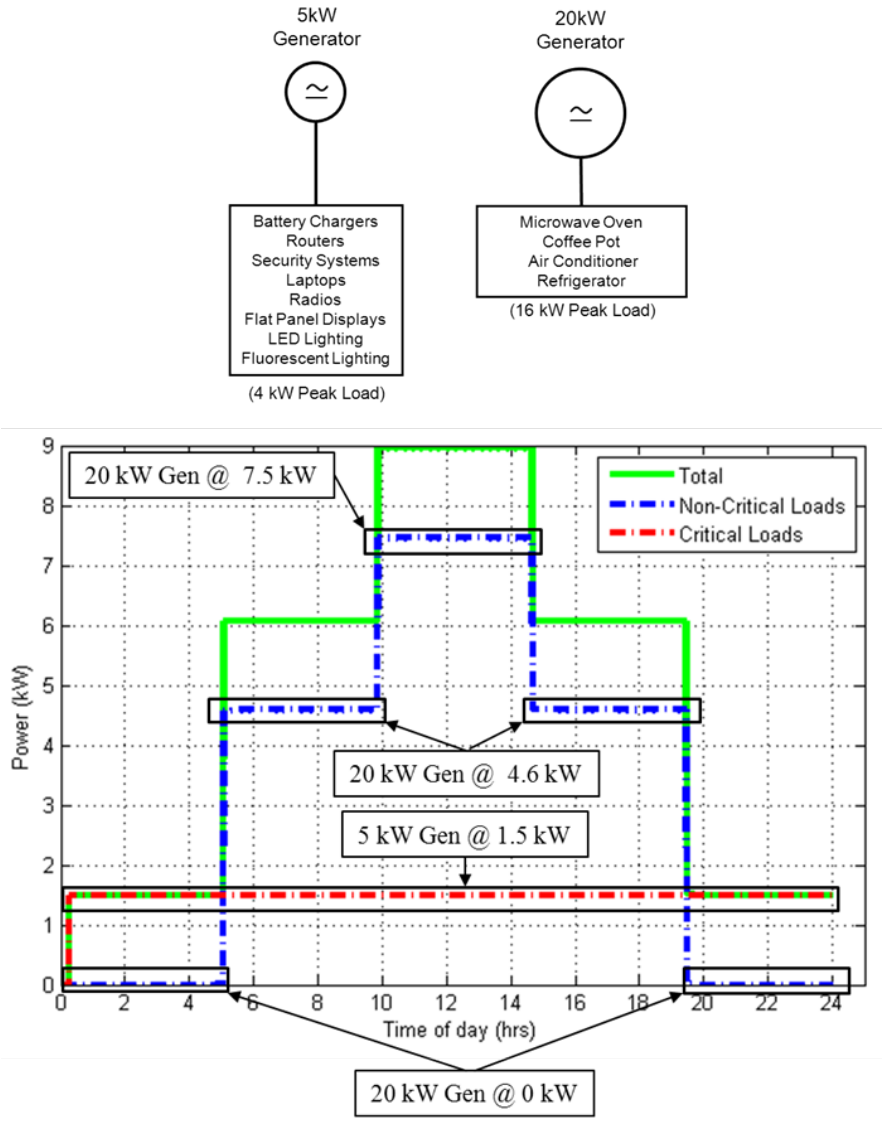

Figure 5. Traditional two-generator handling of the loads.

Table 1. Total generator fuel consumption using traditional method of generator employment.

Power Source	Time of Day	Duration (hrs)	Generator Load (kW)	Generator Operating Point	Fuel Flow (gph)	Fuel Consumed (gal)
5 kW Gen	0000-2359	24	1.5	30.0%	0.251	6.024
20 kW Gen	0000-0500	5	0	0.0%	0.4163	2.0815
	0500-1000	5	4.6	23.0%	0.805	4.025
	1000-1430	4.5	7.5	37.5%	1.05	4.725
	1430-1930	5	4.6	23.0%	0.805	4.025
	1930-2359	4.5	0	0.0%	0.4163	1.87335
					TOTAL:	**22.75385**

The integration of the EMS decreases overall generator fuel consumption while still providing power to the loads. The EMS-enabled scenario is compared to the traditional scenario using the same 24-hour load profile from the traditional scenario presented in Figure 5. Unlike the traditional scenario, the loads are connected to the EMS, not directly to a generator. Critical loads are connected to the EMS's critical bus, and the non-critical loads are connected to the EMS's non-critical bus, as shown in Figure 6. Another difference of the EMS-enabled setup as compared to the traditional method of generator employment is that no more than one generator is used to power the loads at any given time. In other words, for the architecture shown in the top of Figure 6, the EMS may connect to Generator 1, Generator 2, or operate solely on battery power.

Design principles guiding EMS logic are as follow:

- Provide uninterrupted power to critical loads at all times
- Shed non-critical loads when necessary to maintain power to the critical loads
- Use the battery bank to supplement power as necessary
- Utilize the battery bank or the smallest generator possible to supply power to the loads

Logic was developed and implemented in a Simulink model to explore how the EMS handled the notional 24-hour load profile from Figure 5. The results of the simulation determined which power source the EMS selected based upon the total load demand over the 24-hour period. Boxed regions surrounding different portions of the

total load demand are shown in Figure 6. Each region defines the period of time in which the EMS selects a particular power source. An associated numeric label corresponding to each region relates to information contained in Table 2.

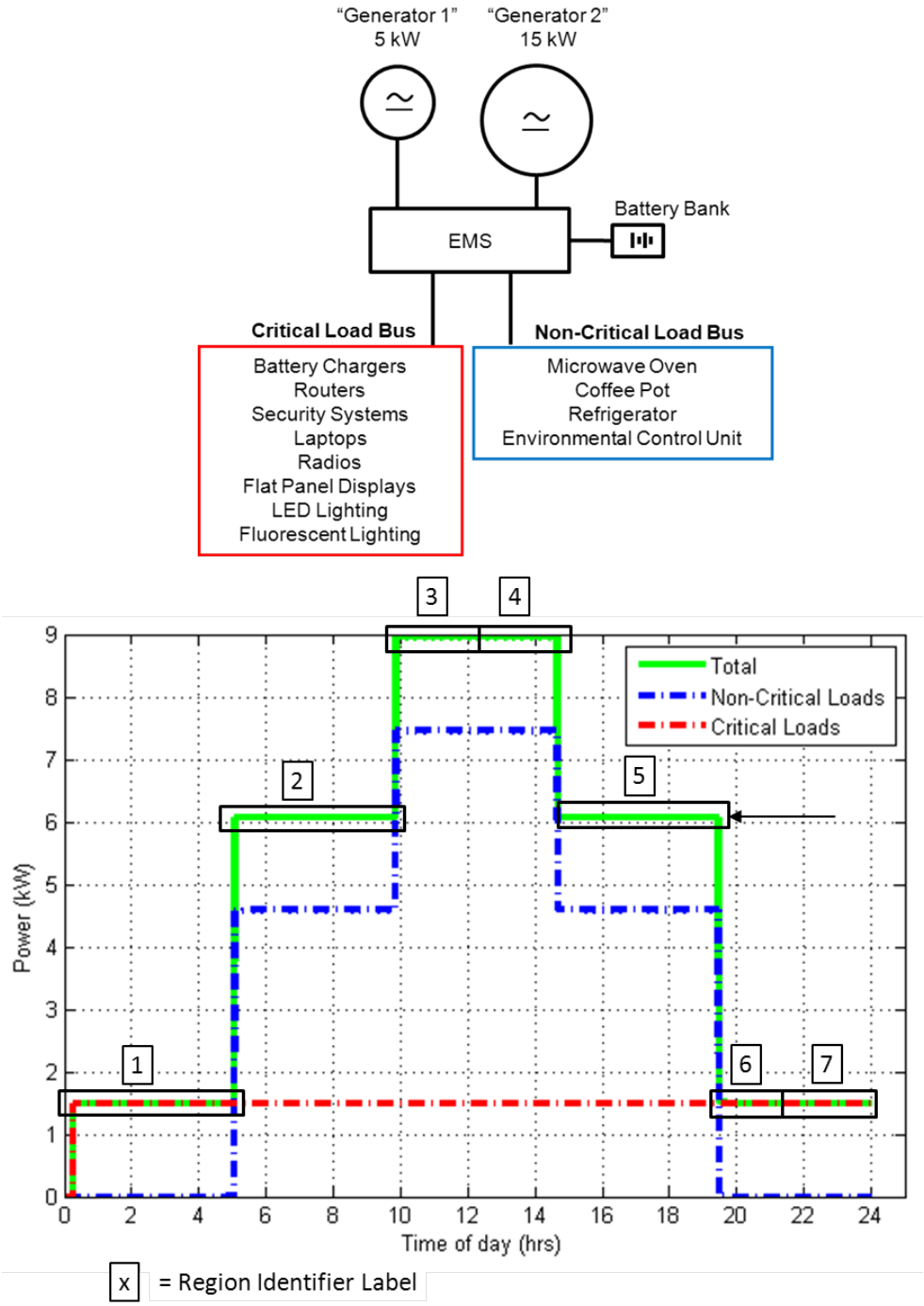

Figure 6. EMS-enabled load handling.

Table 2. Generator selection, loading, and fuel consumption for total load profile in Figure 6.

Region	Selected Generator	Duration (hrs)	Generator Load (kW)	Generator Operating Point	Fuel Flow (gph)	Fuel Consumed (gal)
1	NONE					
2	5 kW	5	5	100%	0.573	2.865
3	15 kW	2.17	15	100%	1.23	2.6691
4	15 kW	2.33	9	60%	0.83	1.9339
5	5 kW	5	5	100%	0.573	2.865
6	5 kW	1.57	5	100%	0.573	0.89961
7	NONE					
					TOTAL:	**11.23261**

It is important to note that the generator load for Region 3 and Region 6 in Table 2 is higher than the total load demand depicted in Figure 6 because during these times the EMS used excess generator capacity to fully recharge the battery bank. In the EMS-enabled scenario, the total fuel consumed by the gas generators was 11.2 gallons over the 24-hour period. This was approximately one-half of the daily fuel consumed by the traditional method of generator employment from Figure 5. The decreased fuel consumption resulted from optimization in a variety of areas. First, the EMS used the battery pack to provide power in times of low loading, meaning the generators were shut off and not consuming any fuel. Second, the battery pack's supplemental power allowed a 15 kW generator to be substituted for the 20 kW generator in the traditional scenario. This was beneficial because the 15 kW generator has a lower fuel flow than the 20 kW generator for a given load. Third, the EMS only operated one generator at a time. The chosen generator was smallest option available that could power the loads while the other generator was shut down. Results from Table 2 show that the generator operating points are as high as 100 percent and are consistently higher than those shown in Table 1 for the traditional method of generator employment.

THIS PAGE INTENTIONALLY LEFT BLANK

LIST OF REFERENCES

[1] R. Tiron, "$400 per gallon gas to drive debate over cost of war in Afghanistan," *The Hill*, [Online]. Available: http://thehill.com/homenews/administration/63407–400gallon-gas-another-cost-of-war-in-afghanistan.

[2] B. Frazee, "Energy symposium looks at reducing the load in Marine Corps expeditionary operations," in U. S. Marine Corps Forces Reserve, February 2010, [Online]. Available: http://www.marforres.marines.mil/MFRNews/NewsArticleDisplay/tabid/7930/Article/81664/.

[3] "Hybridization tradeoffs," Naval Sea Systems Command (NAVSEA) Warfare Centers Carderock, U. S. Navy, Bethesda, MD.

[4] E. Shields, B. Newell, "Current power and energy requirements of forward Deployed USMC Locations," Released January 2012, Quantico, VA.

[5] "Approximate diesel fuel consumption chart" [Online]. Available: http://www.dieselserviceandsupply.com/Diesel_Fuel_Consumption.aspx.

[6] "E2O update, Nov 2011," USMC Expeditionary Power Systems, U.S. Marine Corps.

THIS PAGE INTENTIONALLY LEFT BLANK

ACKNOWLEDGMENTS

I give my appreciation to my thesis advisors, Dr. Oriti and Dr. Julian, for their inspiration and guidance throughout the development of my thesis. I also thank the Department of Computer and Electrical Engineering faculty and staff for their patience in classroom, assistance in the laboratory, and positive impact on my academic success. I extend a grateful acknowledgement to the library staff for the vital support they provided, and to the thesis processors for their commitment to excellence.

To my wife, Nikki, I give you my sincere thanks for your unwavering support. I share my achievements with you.

THIS PAGE INTENTIONALLY LEFT BLANK

I. INTRODUCTION

A. BACKGROUND

A Marine Corps Forward Operating Base (FOB) is a self-contained military base designed to support combat operations in an austere environment often without pre-existing infrastructure. Similar in function to a permanent military base, a FOB contains planning spaces, billeting tents, and a variety of equipment, which all require electricity. However, lacking a utility grid the primary source of a FOB's electrical power is provided on-site by diesel generators.

Marines and soldiers are responsible for the transportation, safe employment, maintenance, and re-fueling of forward-deployed generators. These efforts enable sustained generator operation but also impose significant logistical challenges to deployed forces. For instance, the cost of fuel alone is a tremendous financial burden to the Department of Defense (DoD) at an estimated $400 per gallon delivered to a FOB [1]. In addition to the high dollar cost of fuel, the necessity of resupply convoys to deliver the fuel pose significant risk to U.S. armed forces. Former Commandant of the Marine Corps General James Conway related that 10–15 percent of Marine casualties occur during fuel and water convoy operations alone [2].

The energy profile of for a typical FOB is presented in [3]. Its energy demand by category is summarized in Figure 1. The majority of electrical energy is consumed by environmental control units (ECUs), which are used to heat or cool ambient air in the billeting spaces or the combat operations center (COC). The next largest electrical load is presented by the Ground Based Operational Surveillance System (GBOSS). Other loads, such as lighting or computers, collectively represent only 10 percent of the total energy demand.

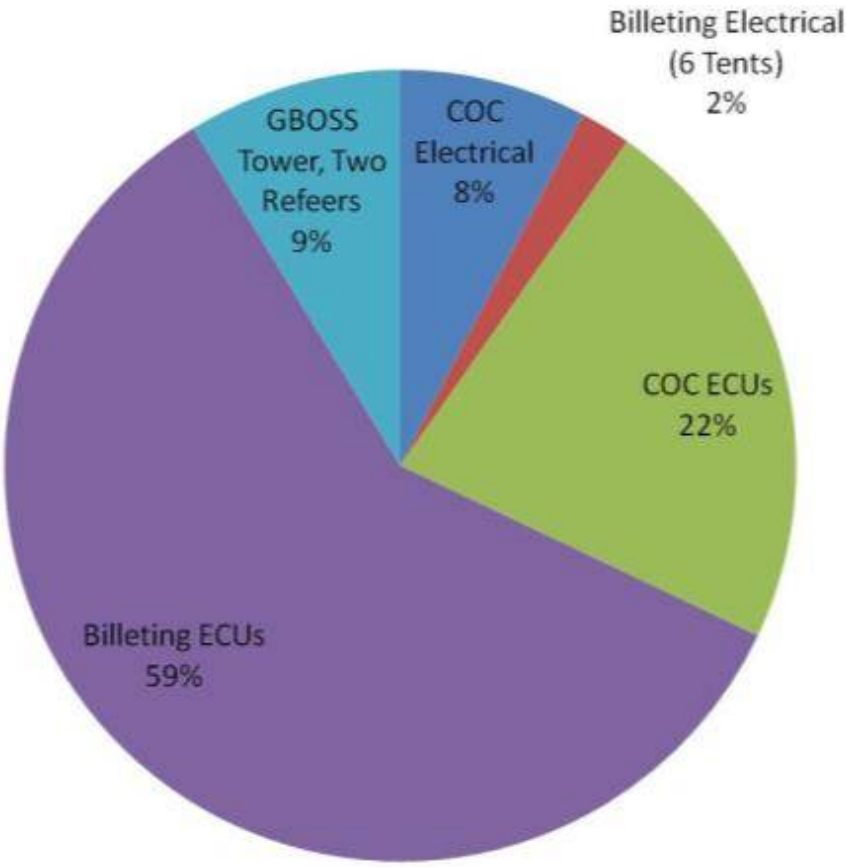

Figure 1. FOB electrical distribution. From [3].

B. OBJECTIVE

More efficient generator use presents an opportunity to reduce a FOB's overall fuel consumption and, in turn, save money while reducing risk to American troops. An internal combustion engine, whether it powers an automobile or an electrical generator, has varying fuel efficiency depending upon the load it drives. For example, a car owner may notice that his vehicle achieves the highest fuel efficiency (in terms of miles traveled per gallon) when driving at a particular speed, perhaps 55 miles per hour. In this case, the vehicle's fuel efficiency is related to its speed assuming all other factors such as terrain or wind remain equal. In a similar manner the efficiency of a diesel generator is related to its electrical power output as shown in Figure 2 for an example 10 kW tactical quiet generator (TQG).

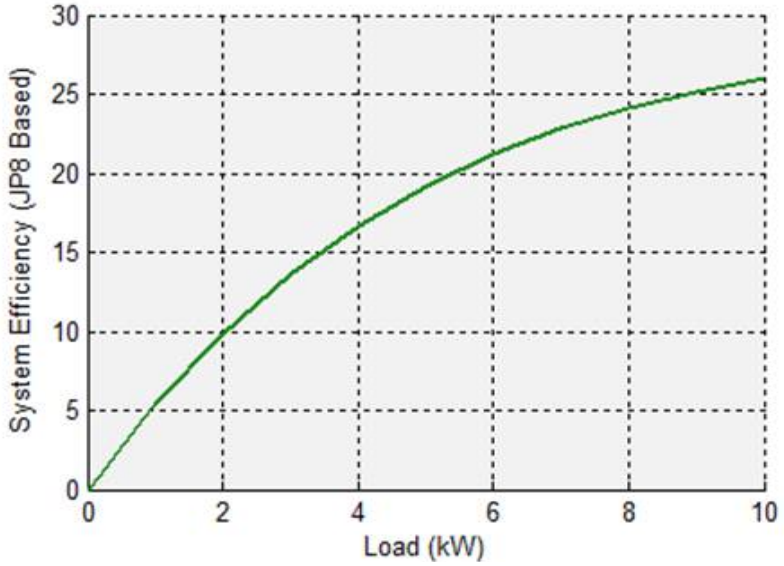

Figure 2. Efficiency of a 10 kW generator versus load. After [4].

One measure of a generator's efficiency relates the electrical power delivered to the load per quantity of fuel consumed by

$$\text{Generator Efficiency (W/gal)} = \left(\frac{\text{Power Delivered to Load}}{\text{Quantity of Fuel Consumed}} \right) \tag{1}$$

where the power delivered to the load is measured in Watts and the quantity of fuel is in gallons. A generator's *operating point* is given by

$$\text{Operating Point (\%)} = \left(\frac{\text{Actual Load}}{\text{Maximum Rated Load}} \right) 100\% \tag{2}$$

where the operating point is the generator's load expressed as percentage of its total capacity.

Some inferences can be drawn from Figure 2 by analyzing the relationship between generator efficiency and operating point. First, at no load the efficiency of the generator is zero. This makes sense because although the generator is not delivering power to a load its engine is still idling and consuming fuel. Second, the generator's maximum efficiency occurs at a 100 percent operating point. Finally, the generator's

efficiency monotonically increases as its operating point (or loading) increases. For the purpose of this thesis the aforementioned inferences are assumed to apply to the range of TQGs fielded by the United States Marine Corps (USMC).

The EMS functionality developed in this thesis allows the EMS to choose between two differently rated generators or a battery bank as the primary source of electrical power. The objective of this thesis is to introduce an EMS into the FOB power system in order to more efficiently utilize generators and reduce overall fuel consumption. This goal is accomplished by ensuring that the EMS chooses the smallest generator capable of powering the load as the primary power source so that the generator operates at high efficiency. Additionally, the EMS has the option of using energy stored in a battery pack and shutting down all generators during periods of light loading. Generator rating, battery bank state of charge (SoC), and real-time power demand all factor into the source selection decision.

C. RELATED WORK

The EMS provides an electrical interface between gas generators, renewable sources, energy storage elements, and loads. Power electronics and digital logic provide key underlying technologies that enable the EMS to measure and control the flow of power between connected elements [5–6]. Solid state systems have been developed and analyzed for applications ranging from peak power control to direct current power distribution to control of power in autonomous microgrids [7–10]. Already, the Marine Corps has integrated solar panels and batteries into some FOB power systems [11], reinforcing the need for a power management solution that can integrate all aspects of the microgrid to include generators and loads.

D. THESIS ORGANIZATION

A small-scale hardware-based experiment is introduced in Chapter II to verify that the EMS can successfully transfer from an external power source to its H-bridge inverter and then back to an external voltage source. Next, a physics based model of the EMS is implemented in Simulink, and the results of the simulation are verified against those of the laboratory experiment.

Two methods of generator employment are explored in Chapter III. The first method is considered traditional, wherein two generators are each connected to a set of loads and operate independently from one another. The second method uses the EMS as the common point of connection between both generators, their loads, and a battery bank, forming a microgrid. EMS logic dictates which power source serves the loads under the microgrid architecture. Design considerations guiding EMS development are introduced, as well as those factors that influence system operation such as load demand, generator rating, and the composition and capabilities of the battery bank.

An example scenario is used in Chapter IV to demonstrate how the EMS manages available power sources as a function of load demand. In this scenario a 24-hour power profile is presented showing the power demanded by two sets of loads and the resulting total power requirement. The 24-hour scenario is scaled down to a 1.5 second version and applied to a model of the EMS created in Simulink. Important systems states are analyzed in detail throughout the simulation and include the status of generator connections, supplemental power from the battery bank, and non-critical load bus shedding.

The total fuel consumed by the generators in both the traditional and EMS-enabled architectures is compared in Chapter V. The 24-hour load profile from Chapter IV is applied directly to the traditional generator scenario. For the EMS-enabled architecture, the results of the Simulink model from Chapter IV are used to determine which generator is operating at any given time. The fuel consumed by each generator in either scenario is calculated from the particular generator's operating point and its corresponding fuel flow. The sum of all the fuel quantities consumed throughout the day is compared to confirm the thesis that the EMS-enabled microgrid architecture reduces fuel consumption as compared to traditional generator employment.

THIS PAGE INTENTIONALLY LEFT BLANK

II. LAB EXPERIMENT AND MODEL VALIDATION

A. EMS FUNCTIONALITY

The EMS provides an interface between the loads, conventional and renewable power sources, and energy storage elements, as shown in Figure 3. The EMS has the potential to carry out many useful functions applicable to today's power management needs. These capabilities include peak power management, uninterrupted power to critical loads, automatic power source selection, and selective load shedding. The functionality demonstrated in this chapter focuses on the EMS's ability to transfer from one power source to another while providing uninterrupted power to the load.

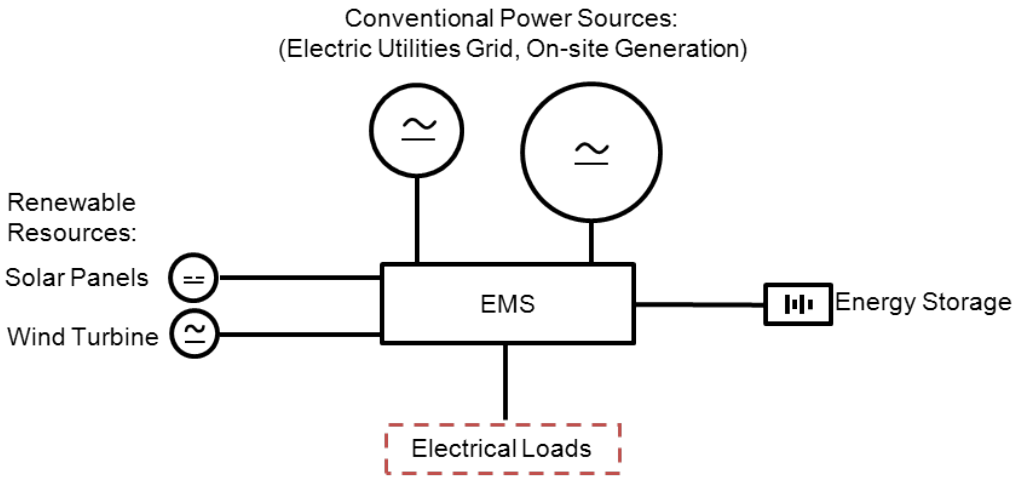

Figure 3. Diagram of EMS interconnections.

B. EMS DESIGN AND HARDWARE

A small scale laboratory experiment conducted to demonstrate the EMS's ability to transfer from one voltage source to another while maintaining current to the load is presented in this section. The electrical schematic depicting the experiment is shown in Figure 4, where $V_{sA}=V_{sB}=116\ V_{rms}$, $L_{sA}=L_{sB}=300\ \mu H$, $L_{fil}=1160\ \mu H$, $C_{cfil}=12\ \mu F$, and the load is a 400 Ω resistor. The EMS includes a battery pack, boost converter, and H-bridge inverter, which are depicted within the boxed region in Figure 4.

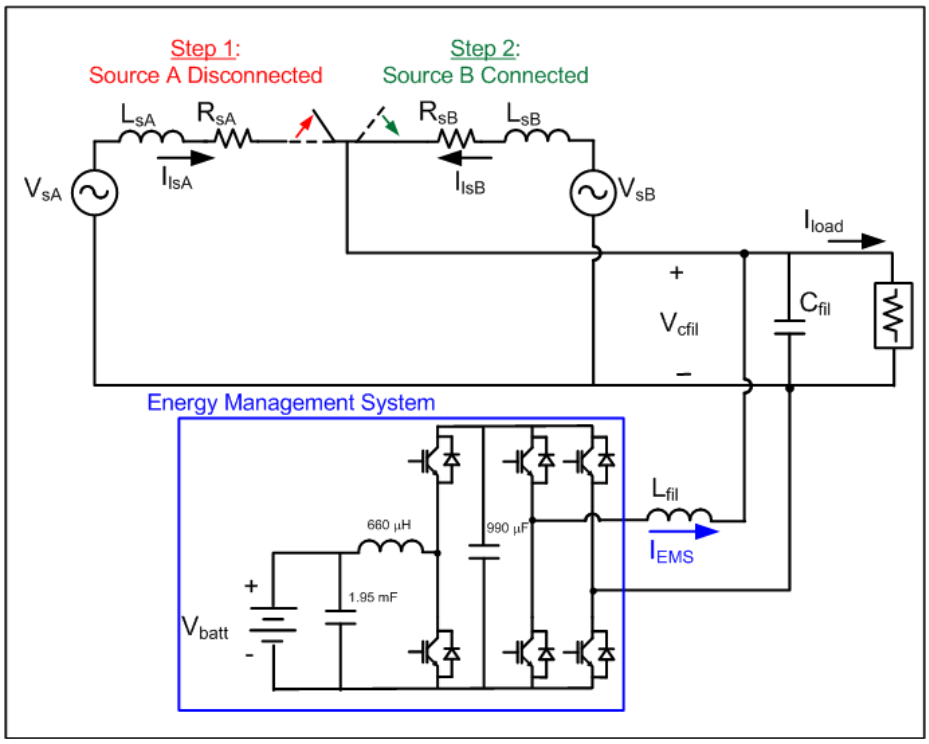

Figure 4. Schematic of experimental setup.

The hardware on the laboratory workbench is shown in Figure 5 including, from the bottom of the stack, a power conversion custom printed circuit board (PCB), field-programmable gate array (FPGA) development board and signal processing board. The battery pack is visible on the left hand side.

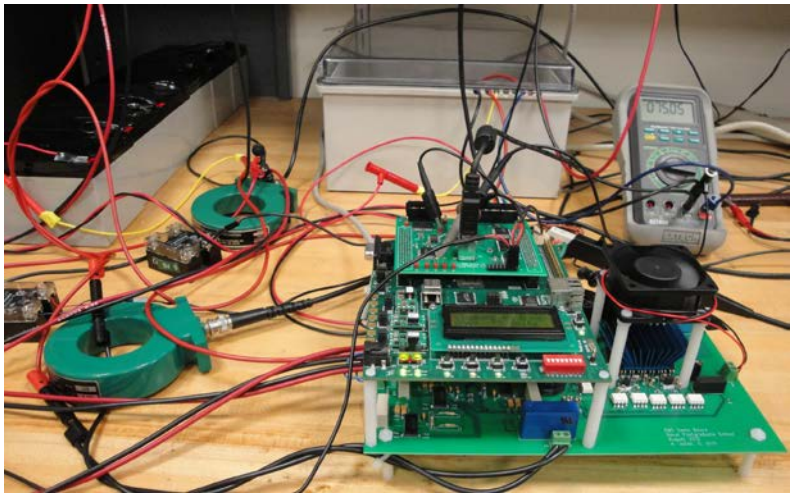

Figure 5. EMS set up in the lab.

A block diagram illustrating the EMS's functional components and interconnections is shown in Figure 6. The EMS logic was implemented on a personal computer (PC) using Simulink's standard features and an additional Xilinx toolbox. The blocks on the right-hand side of the Figure 6 represent the EMS's inputs. The PC communicates with the FPGA through a universal serial bus (USB) port and an interface chip. The Simulink code was loaded from the PC onto the FPGA using Xilinx's System Generator software. A program called Chipscope was used to manually control desired signals transferred between the FPGA and functional components on the PCB. The major functional EMS components are contained in the large rectangle in the center of the diagram, which represents the PCB. In addition to sending user-defined inputs from Chipscope, the logic embedded on the FPGA is also used to control the EMS. Sensors on the PCB make voltage and current measurements of connected devices and relay this information to the FPGA through an analog-to-digital (A/D) converter. The FPGA processes signals using embedded logic and sends control signals to the functional components on the PCB. These components include the insulated gate bipolar transistor integrated power module (IGBT IPM), transistor-to-transistor logic (TTL) interface, and liquid crystal display (LCD). The IGBT IPM enables the EMS to control the flow of power between the AC voltage source and H-bridge converter. Signals from the TTL interface connect or disconnect loads using relays. Information, such as real-time voltage or current measurements, is displayed on the LCD.

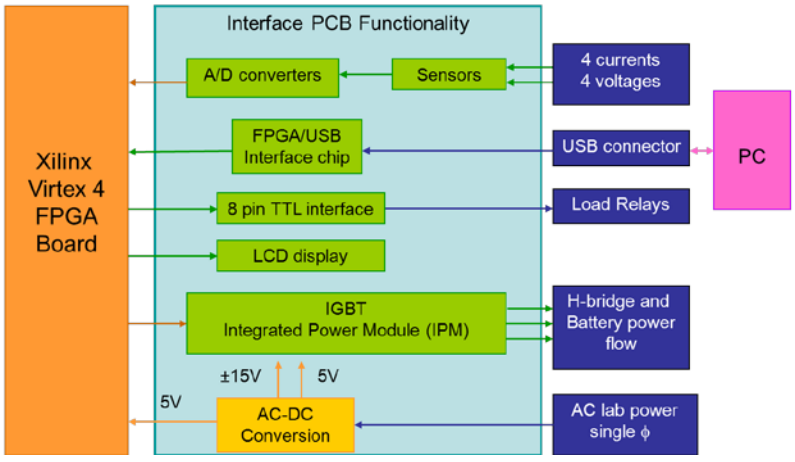

Figure 6. EMS electronics diagram.

For the laboratory demonstration, the switching events depicted in Figure 4 were manually commanded. First, the source V_{sA} was disconnected from the load. The current and voltage waveforms produced during the transition from V_{sA} to the EMS as a voltage source are depicted in Figure 7. At 75 ms, the moment of the disconnect event, the EMS current stepped from 0 to 270 mA_{rms} as the EMS provided uninterrupted in-phase current to the load. In this experiment the EMS was programmed to produce a slightly lower voltage V_{cfil} than that of the grid. This allowed easy visual identification of the switching events depicted in Figure 7 and Figure 8.

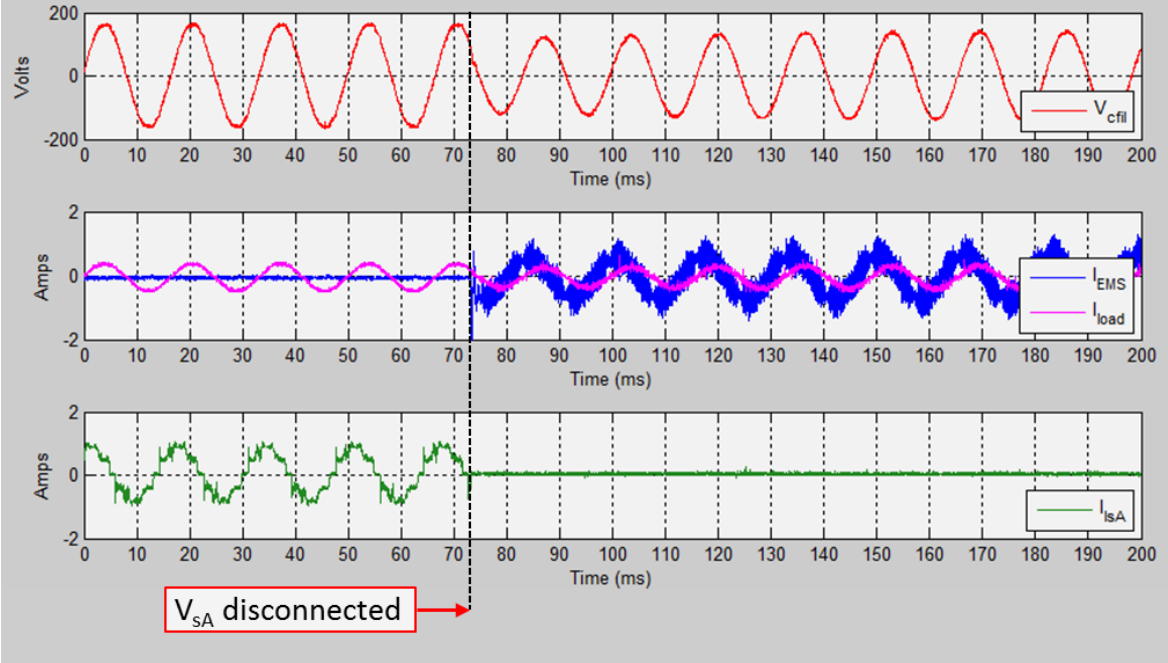

Figure 7. Experimental voltage and current measurements when V_{sA} is disconnected.

Next, the second power source, $V_{sB,}$ was connected to the load. The current and voltage waveforms produced during the transition from the EMS to V_{sB} are depicted in Figure 8. At 73 ms, the instant when V_{sB} was connected, I_{ls} increased from 0 A to 270 mA_{rms}, and I_{EMS} dropped to 0 A. During this transition the load continued to receive uninterrupted in-phase current as shown by the I_{load} waveform in Figure 8.

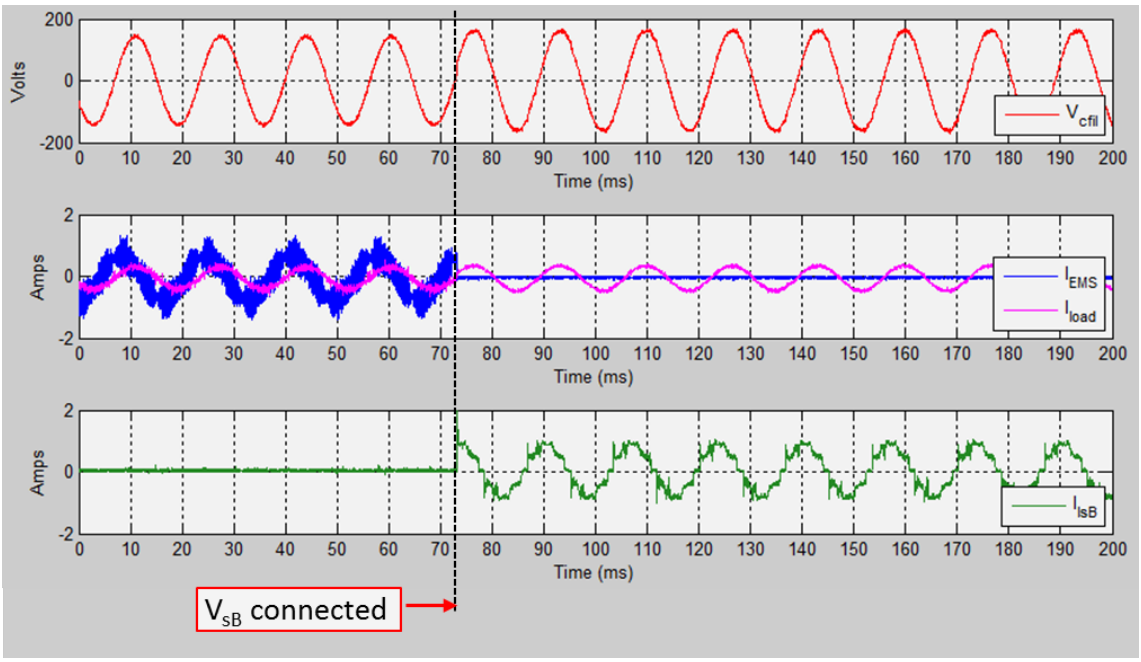

Figure 8. Experimental voltage and current measurements when V_{sB} is connected.

C. MODELING THE EMS IN SIMULINK

The EMS physics based model was implemented in Simulink, and then the results of the simulation were compared to those obtained in the laboratory experiment. The top level of the model is depicted in Figure 9. The most significant features of the EMS hardware were taken into consideration when designing the Simulink® model. The sources V_{sA}, V_{sB} and the H-bridge reference voltages were made in phase with one another for ease of modeling. In reality voltage sources are non-ideal and their frequencies drift slightly from the desired frequency. Therefore, the relative phases of two similar frequency voltage waveforms drift closer and farther apart over time. Eventually, the phase difference becomes so minimal that we consider two waveforms to be momentarily in phase. At this point a phase-locked loop could be used to synchronize the two voltages, or a switch could be closed to transition seamlessly between one voltage source and the other. By modeling the voltage sources in phase with one another, we get the same result, an in-phase voltage transition, without introducing the complexity of frequency drift or phase-locked loops.

The switches used to connect or disconnect V_{sA} and V_{sB} from the EMS are modeled as thyristors where the EMS provides the gate signals. For this simulation we wanted to disconnect V_{sA}, operate the EMS in island mode, and then connect to V_{sB}. For the purposes of this thesis, the term 'island mode' refers to the state of the EMS when it is disconnected from a generator. The thyristor was turned on at a V_{cfil} zero crossing in order to minimize power dissipation when the switch is closed. The thyristor can only turn off when current stops flowing through it, which corresponded to a zero crossing of source current I_{sA} or I_{sB} in our model. The same voltage source, labeled Generator 1 in Figure 9, was used to represent both V_{sA} and V_{sB}. The H-bridge inverter produced a constant 110 V_{rms} in island mode and did not supplement any current when the EMS was connected to a voltage source.

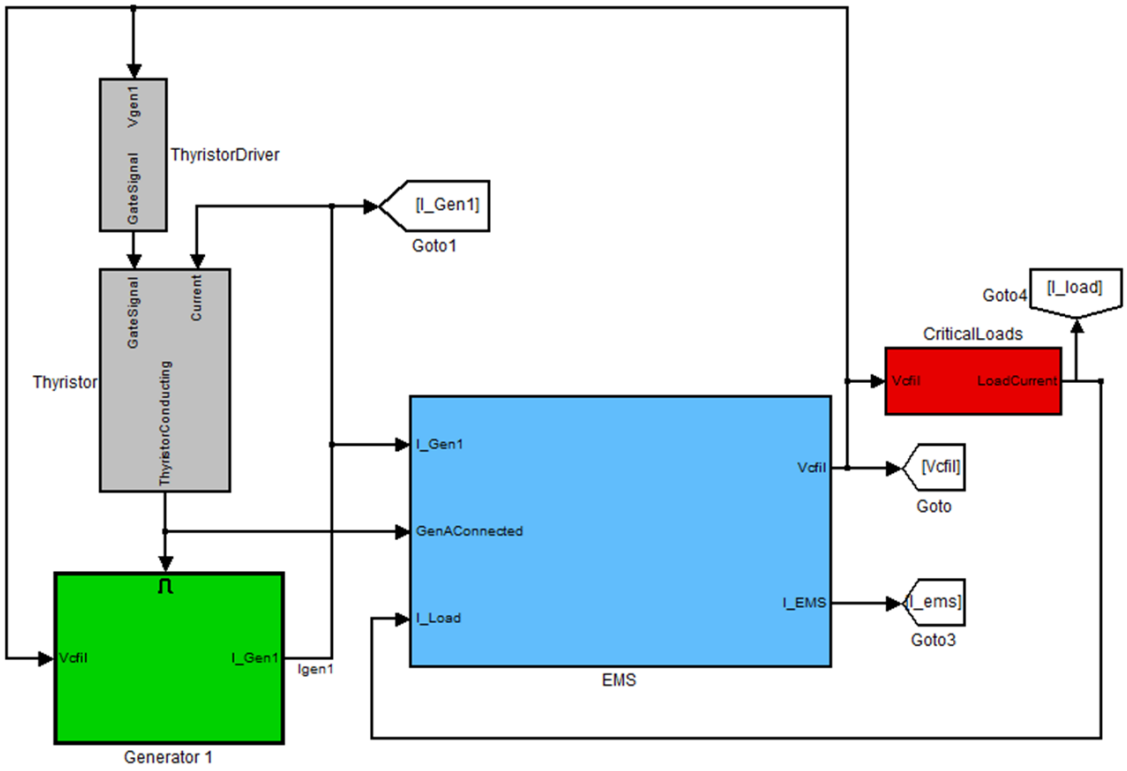

Figure 9. Simulink model used to validate the lab experiment.

The current and voltage waveforms produced by the simulation when V_{sA} was disconnected are shown in Figure 10, and the simulated results when V_{sB} was connected

are shown in Figure 11. These simulated waveforms compare favorably with those produced by the lab experiment in Figures 7 and 8, validating the Simulink model. In the simulation, we disconnected V_{sA} at approximately 100 ms, shown in Figure 10. As with the experimental results from Figure 7, the EMS operated as a voltage source when we disconnected V_{sA} and provided uninterrupted, in-phase, current to the load. We designed the model such that when the EMS was in island mode it produced a slightly lower output bus voltage as compared to when it was connected to a voltage source in order to reflect the EMS's similar operation in hardware.

During the transition from island mode to grid-connected mode the simulated results from Figure 11 aligned well to the lab results shown in Figure 8. In the simulation we connected V_{sB} to the EMS at 92 ms. Once connected to V_{sB}, the EMS ceased operating as a voltage source and the injected current I_{EMS} went to zero. The output bus voltage V_{cfil} rose slightly from the island mode voltage of 110 V_{rms} to the grid voltage of 116 V_{rms}.

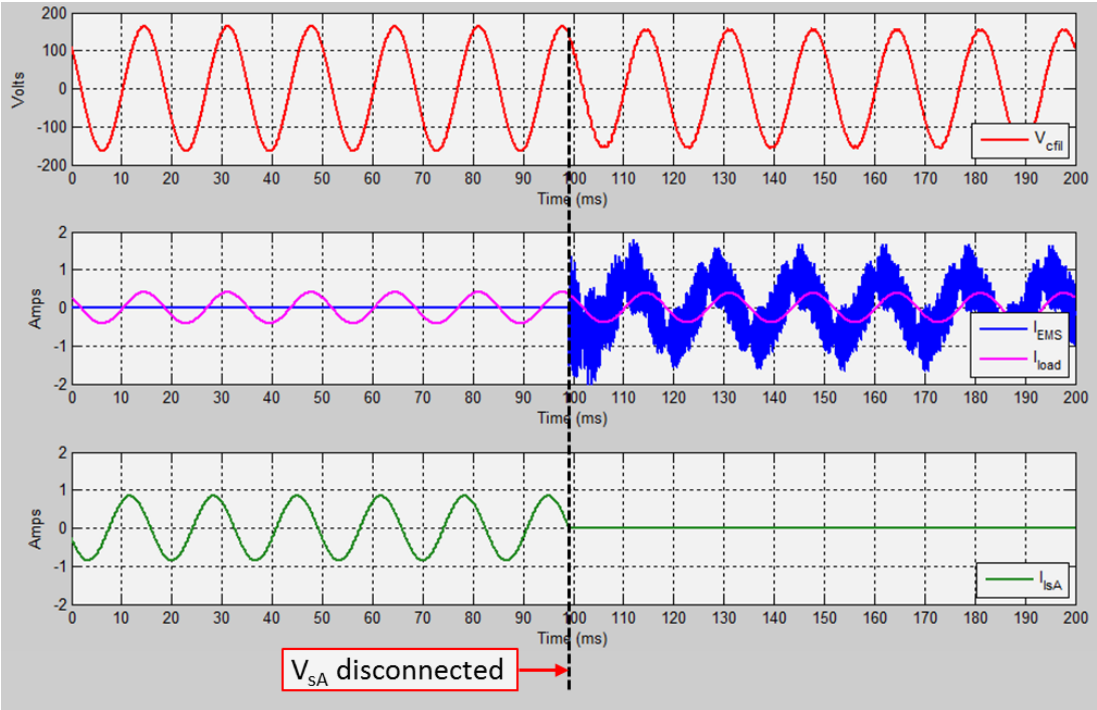

Figure 10. Simulated voltage and current measurements when V_{sA} is disconnected.

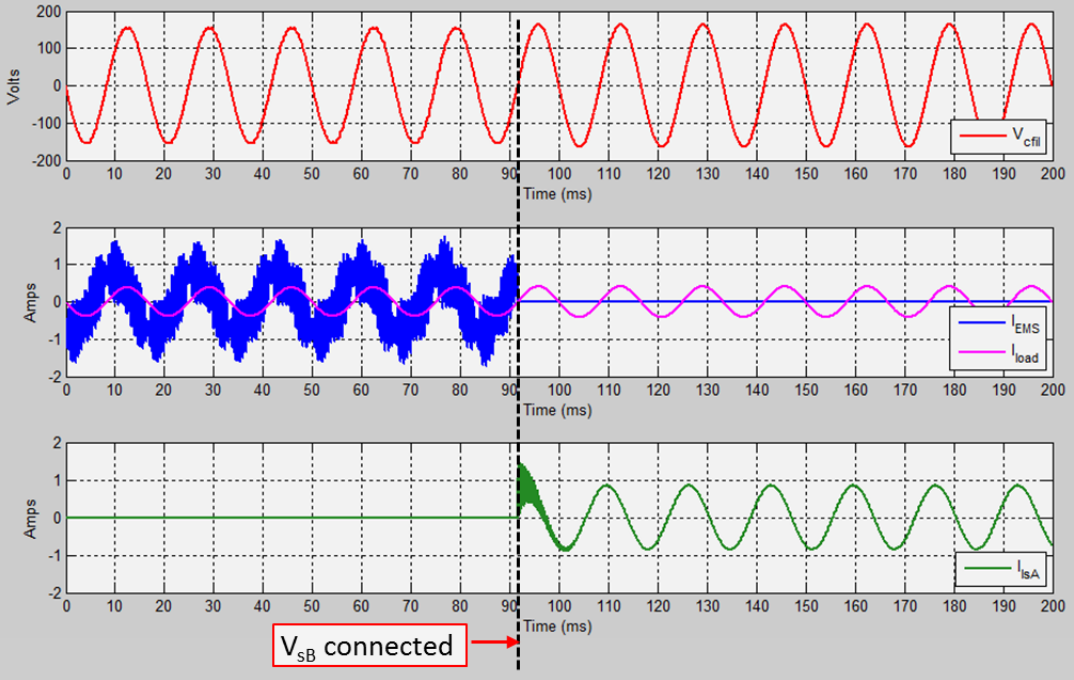

Figure 11. Simulated voltage and current measurements when V_{sB} is connected.

D. CHAPTER SUMMARY

A small-scale hardware-based experiment was conducted to verify that the EMS could successfully transfer from an external power source to its H-bridge inverter in island mode and then back to a voltage source. The results confirmed that the EMS was able to provide uninterrupted power to the load using either source and throughout the handoff events. Next, a physics based model of the EMS was developed and implemented in Simulink. The model produced voltage and current waveforms in Figures 10 and 11, which replicated those from the lab experiment in Figures 7 and 8.

III. EMS FUNCTIONALITY

A. DESIGN PRINCIPLES

Traditionally, generators are connected directly to sets of loads or power distribution buses such that a generator supplies power to its loads independently from other generators and loads [3]. This traditional architecture is illustrated in Figure 12 for two generator-load nodes. The generators operate continuously, and their power demand fluctuates depending upon the operational state of connected loads.

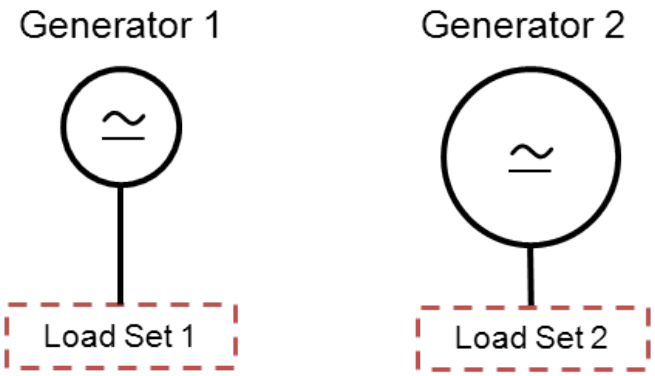

Figure 12. Two generator and load nodes.

An alternative method of connecting loads to power sources is by using the EMS. This configuration, shown in Figure 13, allows the EMS to make power source selection decisions based upon programmable logic, real-time load power demand, and battery bank state of charge.

The design principles for EMS employment are to:

- Provide uninterrupted power to critical loads at all times
- Shed non-critical loads when necessary to maintain power to the critical loads
- Use the battery bank to supplement power as necessary
- Utilize the battery bank or the smallest generator possible to supply power to the loads

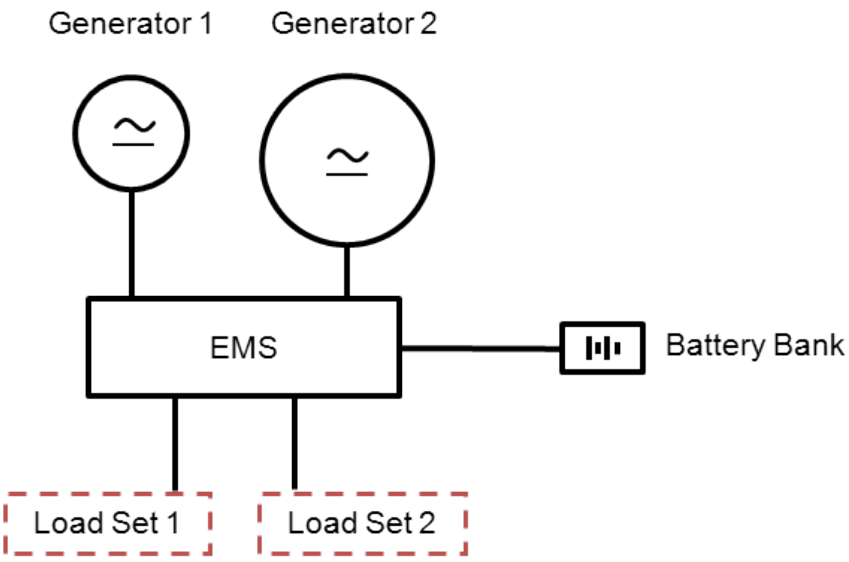

Figure 13. Combined loads connected to the EMS.

For the EMS-based design, loads were categorized into two categories, non-critical and critical. A non-critical load is one that may be turned off for a short period of time with minimal impact to its user. For example, we consider a refrigerator a non-critical load because it can be turned off for 60 seconds without significantly impacting the temperature of the food inside. Air conditioners or ECUs are also non-critical and can be shed momentarily with minimal impact on daily business. On the other hand, critical loads include anything that must remain energized in order to satisfy a mission requirement or ensure safety. Allowing the EMS to suddenly secure overhead lighting poses a safety concern, for instance, and disrupting power to a computer can result in data loss or damage. The EMS has two distinct AC buses, one for the critical loads and one for the non-critical. Each of these buses is controlled by a thyristor and supplies 120 V_{rms} AC power to the respective loads.

B. EMS LOGIC

When operating in island mode, the EMS must recognize when the load demand exceeds the battery bank's power capability and take corrective action. One course of action the EMS may take is to connect to a generator. In this case the load demand

dictates whether the EMS will choose the smaller or larger generator. In the unlikely event that both generators have failed, the EMS will shed the non-critical bus in order to preserve power to the critical load bus using the batteries.

Another scenario arises when the EMS is connected to a generator and the load increases above the generator's capacity. Depending on the magnitude of the power deficit, the EMS has several options from which to choose in order to correct the condition. If the battery bank has sufficient capacity the EMS can supplement current through the H-bridge inverter, bringing the power demand of the generator back within its operating capacity. Alternately, if the batteries are discharged or unable to satisfy the power deficit, the EMS can connect to a larger generator, assuming one is available. Before a handoff from one generator to another the EMS must briefly shed the non-critical loads. This step is necessary to ensure that the critical loads continue to receive power when the EMS briefly enters island mode. Once the desired generator is connected the EMS re-enables the non-critical bus and normal operation resumes. If the largest available generator is connected and the EMS cannot satisfy the load demand even with the help of supplemental EMS current, the EMS must shed the non-critical bus to preserve power to the critical loads.

Many variables and thresholds exist that govern the operation of the EMS in light of the aforementioned scenarios. For example, the battery bank's state of charge determines in part whether or not the EMS can operate in island mode or inject supplemental current. As the batteries discharge, a point is reached where the EMS must recharge them using a generator. Another important consideration is the delay time between EMS logic decisions switching states. Consider the case where the EMS is connected to the larger of two generators, and then assume the load demand increases beyond the generator's capacity even when the EMS injects maximum rated supplemental current. In order to preserve power to the critical loads, the EMS has to shed the non-critical load bus. With the non-critical load bus shed, the power deficit is alleviated. The question remains, though, how long should the EMS wait to attempt re-

connecting the non-critical bus? This question, and many more like it, posed challenges in the design of the EMS logic. In order to organize the major logic decisions, the flow charts shown in Figure 14 and Figure 15 were developed.

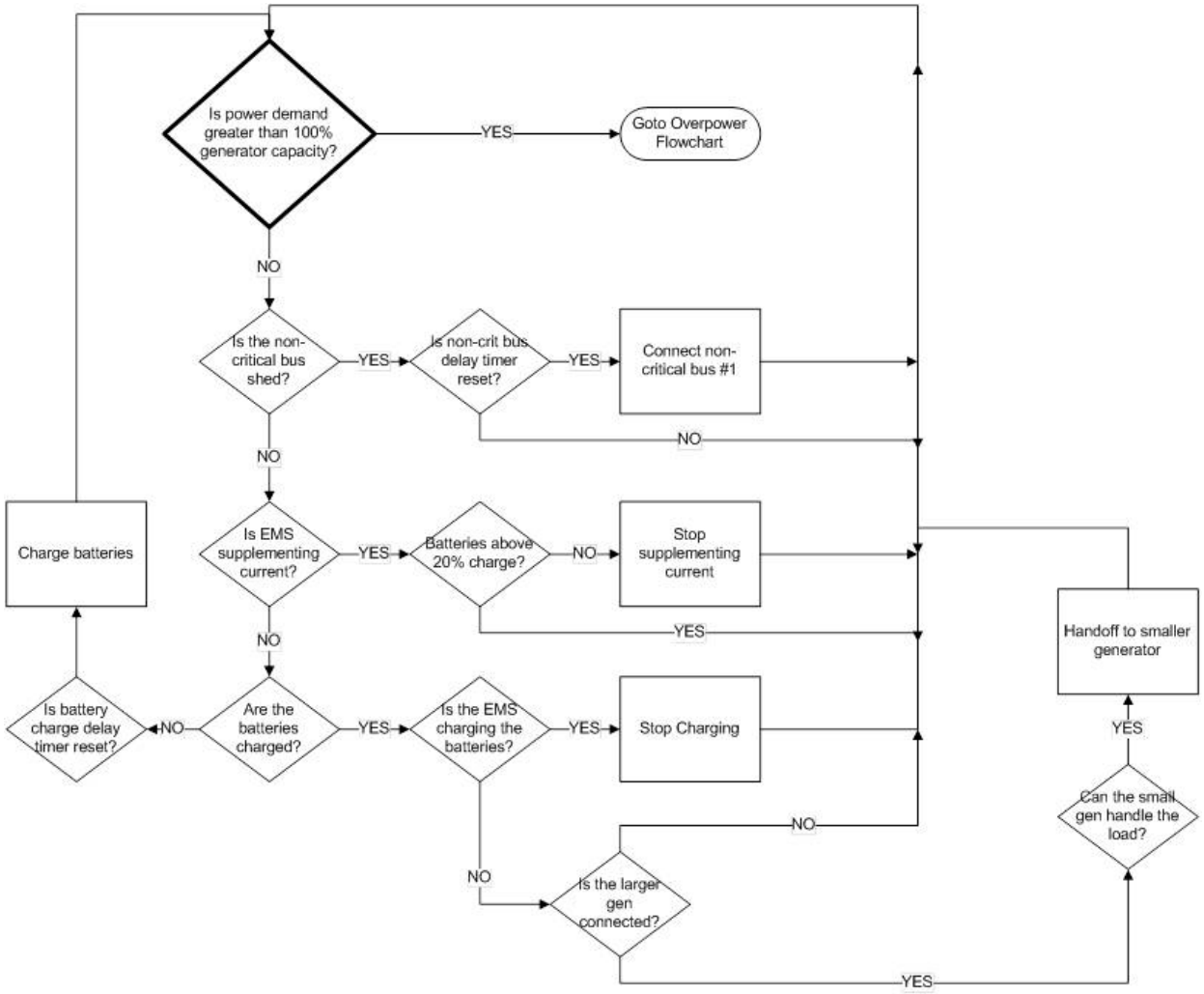

Figure 14. Logic flowchart for EMS when generator is at or below 100 percent capacity.

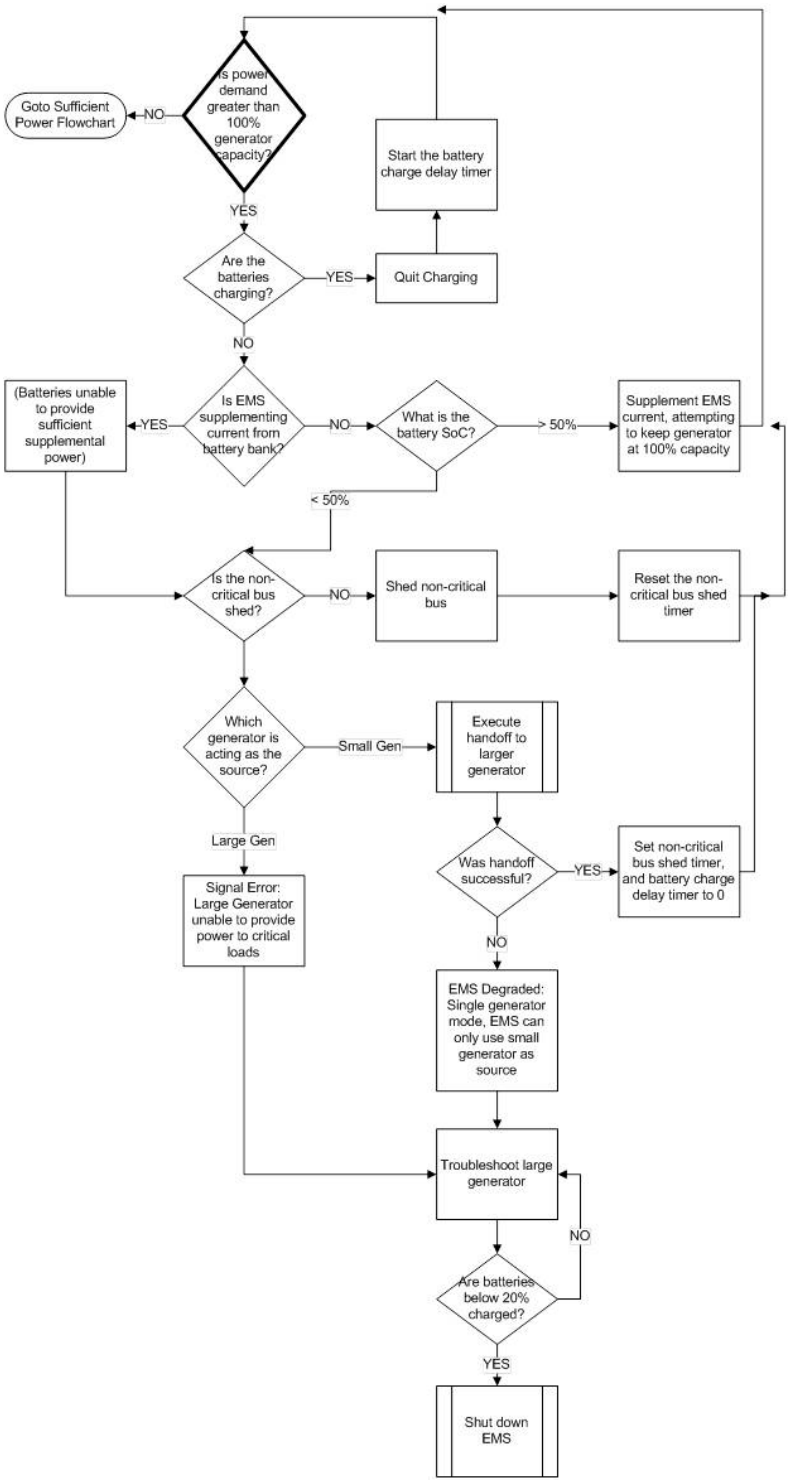

Figure 15. Logic flowchart for EMS when generator is over 100 percent capacity.

C. EMS POWER CALCULATION

One of the primary metrics that influenced the design of the EMS studied in this thesis was the power demand placed upon the source generator. It was necessary that the EMS was able to calculate power flowing from the source generator in real time. Before we determined how the EMS could make this calculation within the context of a complex microgrid, a simpler circuit model facilitated a fundamental understanding power calculation. The circuit presented in Figure 16 contains three elements: an ideal 110 V_{rms} 60 Hz voltage source, a 240 μF capacitor, and a 10 Ω resistive load.

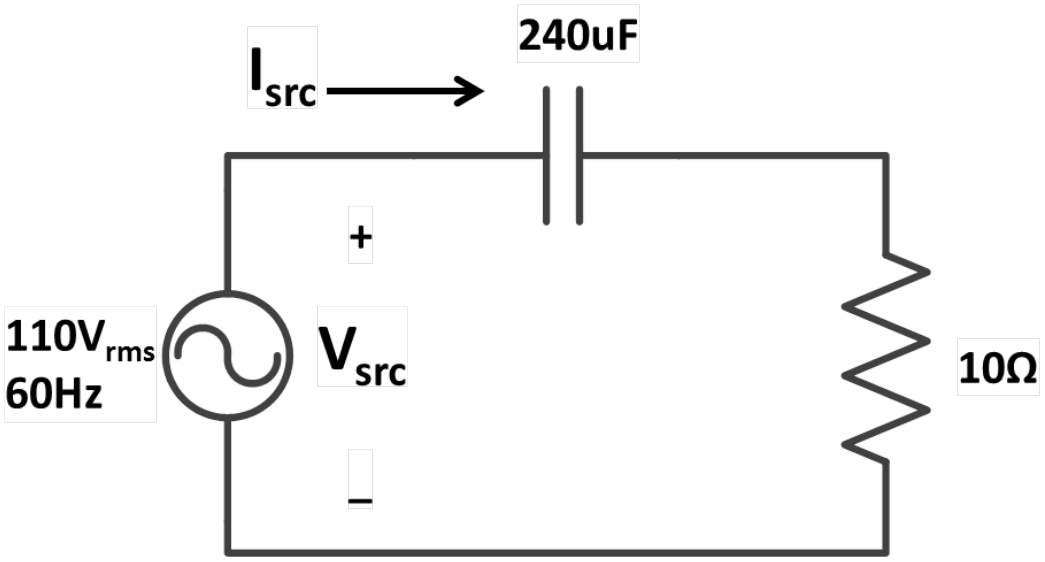

Figure 16. Simple RC circuit

The goal in analyzing the simple resistor-capacitor (RC) circuit was to determine how much real power the voltage source provided. One way of achieving this was to use graphical analysis based upon the voltage and current waveforms produced from the voltage source. The circuit was simulated in the Simulink run-time environment. One cycle of the steady state source voltage and current waveforms is reproduced in Figure 17.

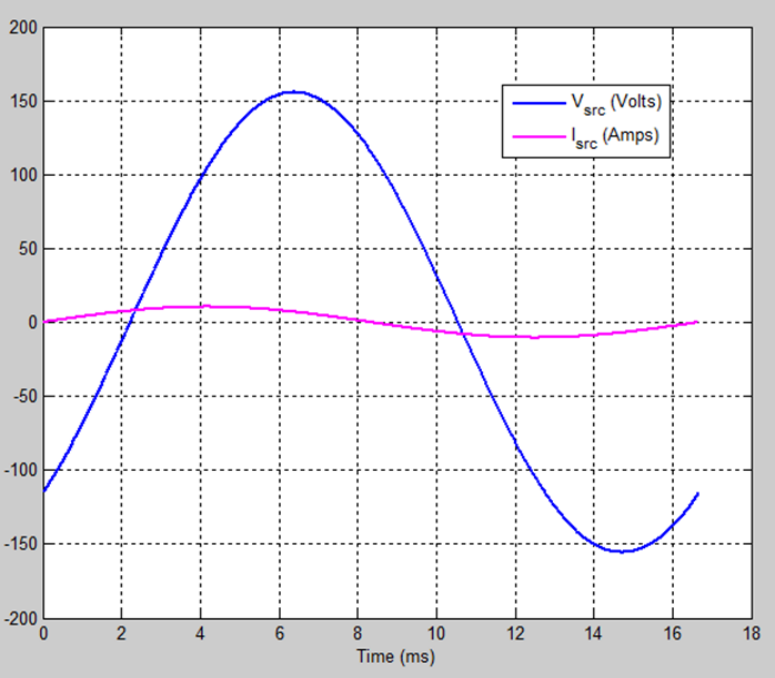

Figure 17. RC circuit source voltage and current.

The voltage and current waveforms in Figure 17 have peak values of 155.5 V and 10.45 A, respectively. Since the V_{src} and I_{src} are pure sinusoids, their respective root-mean-square (RMS) values are given by

$$V_{rms} = \frac{V_{peak}}{\sqrt{2}}, \quad A_{rms} = \frac{A_{peak}}{\sqrt{2}} \tag{3}$$

From Equation 3 the respective voltage and current RMS values are 110 V_{rms} and 7.4 A_{rms}. The voltage and current waveforms are displaced in time by 2.2 ms. We can express this 2.2 ms time difference in terms of a phase angle θ_D by

$$|\theta_D| = (\text{time delay})(\text{frequency})(360°), \tag{4}$$

or for the values from our specific example,

$$|\theta_D| = (2.2\text{ms})(60\text{Hz})(360°) \approx 48°. \tag{5}$$

I_{src} leads V_{src}, therefore θ_D=+48°. The graphical relationship between the magnitudes and angular difference between the current and voltage from Figure 17 is depicted in Figure 18.

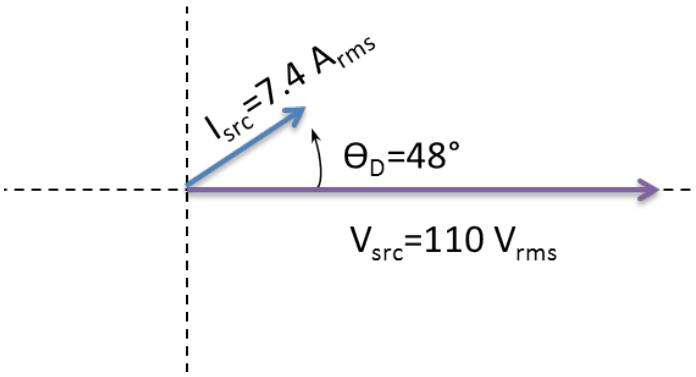

Figure 18. I_{src} and V_{src} with phase angle θ_D.

The real power for the example RC circuit is given by

$$P = V_{rms} I_{rms} \cos(\theta_D), \tag{6}$$

or for our specific example,

$$P = (110 V_{rms})(7.4 A_{rms}) \cos(48°) = 544.7 \text{ Watts} \tag{7}$$

While Equation 6 can only be used for sinusoidal steady state analysis, a more general equation for real power *P*, which correlates to its definition as "average power," is given by

$$P = \frac{1}{T} \int_{t_0}^{t_0+T} i(\tau) v(\tau) d\tau, \tag{8}$$

where *T* is the period in seconds, t_0 is an arbitrary time, $i(\tau)$ is the instantaneous current in amps, and $v(\tau)$ is the instantaneous voltage in volts.

An advantage of Equation 8 over other equations for real power is that RMS and displacement power factor calculations are not required. This becomes especially useful when the current contains frequencies other than the fundamental; in other words, when it is periodic but not sinusoidal. Since the EMS handles currents and voltages that are periodic but are not always purely sinusoidal, Equation 8 was used as the method of real power calculation to implement in the EMS.

The first four cycles of voltage and current for the circuit in Figure 16 are shown in Figure 19. At time zero, we energized the circuit and steady-state operation was reached by the second cycle. The real-time power calculation of real power using Equation 8 is shown in Figure 20.

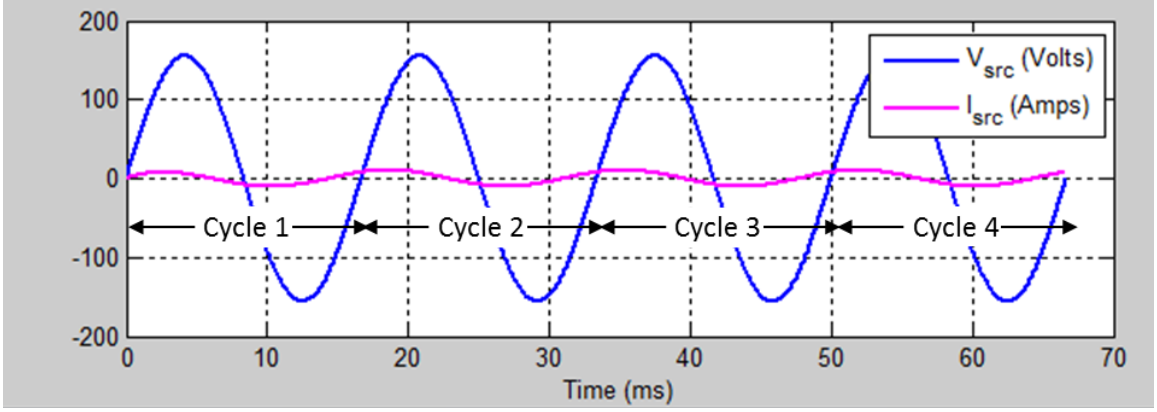

Figure 19. Voltage and current produced by energizing the circuit from Figure 16.

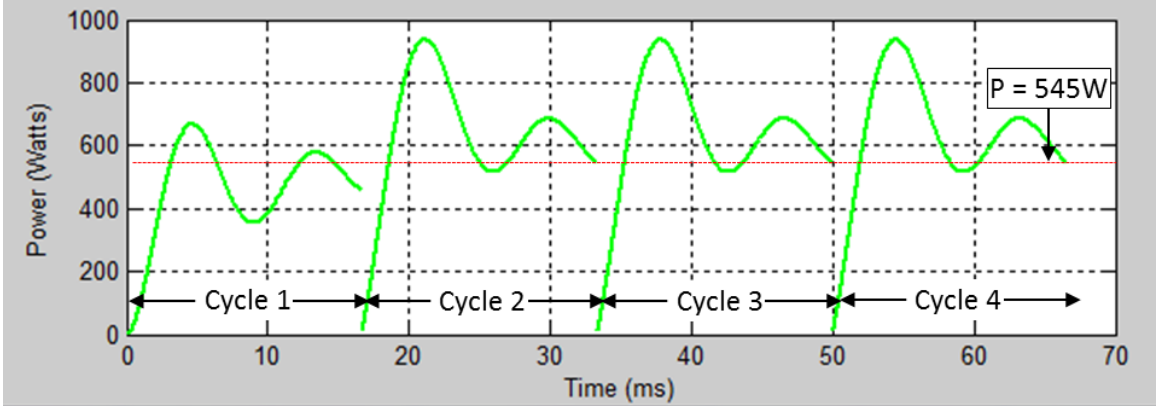

Figure 20. Real-time power calculation for voltage and current from Figure 19.

Notice from Figure 20 that the power measurement converges to the correct value, 545 W, at the end of one time period *T* in steady state operation. To obtain a more useful plot of real power, a sample-and-hold operation is applied at the end of each cycle to create Figure 21.

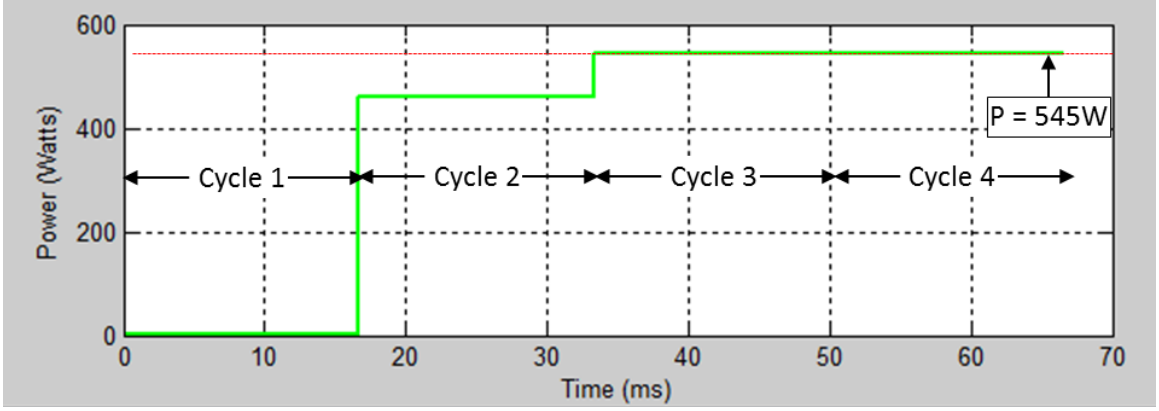

Figure 21. Sample and hold values after each cycle from Figure 20.

The simulation accurately determined the real power flowing through our circuit after each cycle as shown in Figure 21. However, the sample and hold algorithm introduced a one cycle delay. Under transient conditions the real power calculation we implemented in our EMS model adds one cycle time of lag to the circuit's settling time. At a an operating frequency of 60 Hz, one cycle takes 16.7 ms, which we allowed as a tolerable delay terms of EMS design and functionality. The Simulink implementation of the power calculation from Equation 8 is shown in Figure 22.

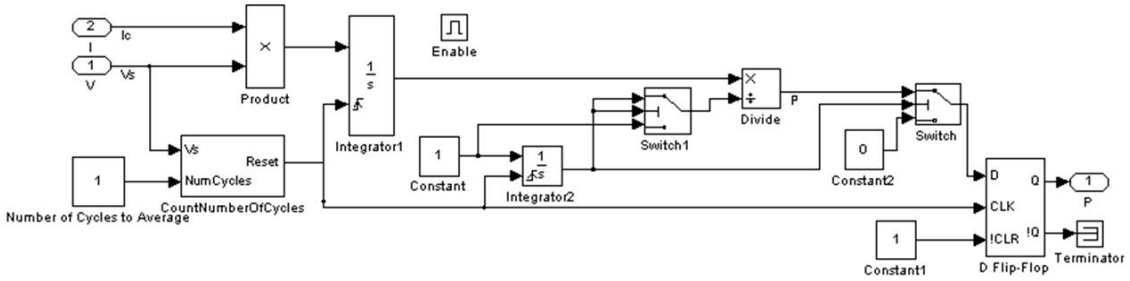

Figure 22. Average power calculation algorithm employed by the EMS model.

D. BATTERY BANK

The EMS can use energy stored in the battery bank to supplement load current when a generator is connected or to potentially provide all of the load power when the EMS is in island mode. Factors such as the battery bank's storage capacity, the maximum

rated battery current, and semiconductor ratings limit the EMS's actual power capability. For the purpose of this model we considered the size of the battery pack as the most significant limiting factor.

1. Battery Technology

Numerous energy storage technologies exist that can serve the purpose of the EMS battery bank. Some of the most widely used technologies are illustrated in Figure 23, which illustrates rated power and discharge time of installed systems.

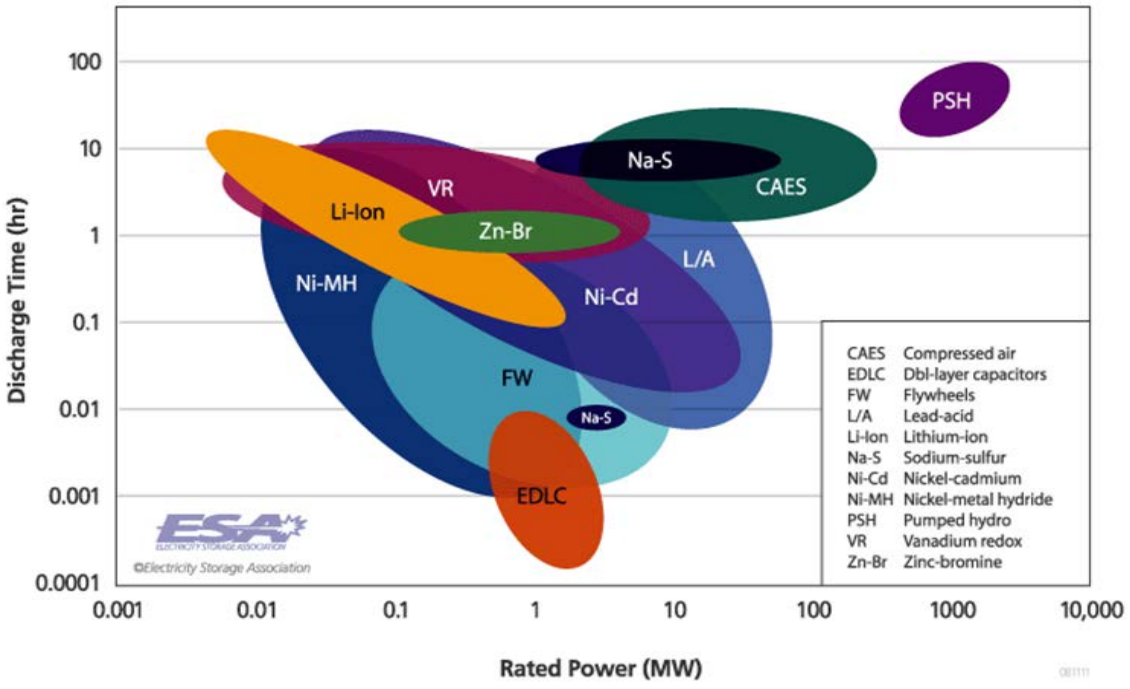

Figure 23. Discharge time and rated power of energy storage technologies. From [12].

Some of the battery choices shown in Figure 23 are lithium-ion, nickel-cadmium, and nickel-metal hydride. These rechargeable batteries have been widely used in portable electronics due to their high energy density. Lead acid batteries, while typically installed in higher-power applications than the EMS, also have desirable characteristics that make them a good choice as the building block of the EMS battery bank. Lead acid batteries

have been used in automobiles for quite some time and are widely available around the globe. In addition, their cost per cycle is comparable to nickel-cadmium and lithium-ion as shown in Figure 24.

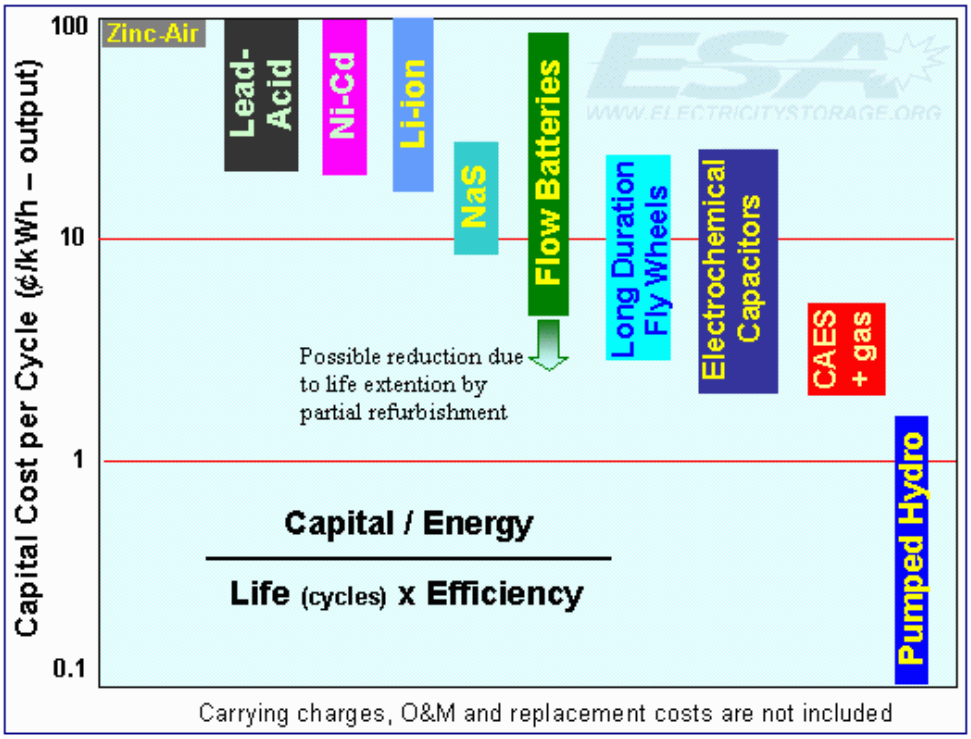

Figure 24. Energy storage technology efficiency over lifetime in cycles. From [12].

A more detailed analysis of competing battery technologies remains a worthwhile endeavor but was outside the scope of this thesis. For the sake of continuing with the study of the EMS in this thesis, the Genesis NP12–12 rechargeable sealed lead-acid battery was chosen as the storage technology of choice based upon our familiarity with them in a laboratory setting.

2. EMS Battery Bank Size and Weight

A portion of the Genesis NP12–12 specification sheet is depicted in Figure 25. Battery capacity, measured in Amp-hours (Ah), is a function of draw time shown in the

specification sheet under the “nominal capacity” heading. It was instructive to estimate the size, weight, cost and other important features of battery bank capable of producing 1 kW of power.

The battery bank design was based upon a maximum of six hours of continuous battery draw time. The rationale behind this decision was based upon the assumptions about what a load profile would look like. It was predicted that the EMS could power the load using batteries alone during times of minimal load demand. It was further predicted that the period of minimal load demand was likely to occur at night when people were sleeping and fewer appliances were operating, and six hours was a conservative time period for how long an average person sleeps.

- **NOMINAL VOLTAGE:** 12V
- **NOMINAL CAPACITY:**
  20 hr. rate of 0.6A to 10.5V 12.0Ah
  10 hr. rate of 1.1A to 10.5V 11.0Ah
  5 hr. rate of 2.1A to 10.2V 10.5Ah
  1 hr. rate of 7.2A to 9.60V 7.2Ah
- **WEIGHT (approx.):** 8.82 pounds (4 kgs.)
- **ENERGY DENSITY (20 hr. rate):**
  1.70 WH/cubic inch (103.5 WH/liter)
- **SPECIFIC ENERGY (20 hr. rate):**
  16.3 WH/pound (36.0 WH/kg)
- **INTERNAL RESISTANCE OF CHARGED BATTERY:**
  16 milliohms (approx.)
- **MAXIMUM DISCHARGE CURRENT WITH STANDARD TERMINALS:**
  40 amperes
- **MAXIMUM SHORT-DURATION DISCHARGE CURRENT:**
  360 amperes
- **OPERATING TEMPERATURE RANGE:**
  CHARGE 5°F to 122°F (-15°C to 50°C)
  DISCHARGE -4°F to 140°F
- **CHARGE RETENTION (shelf life) at 68°F (20°C):**
  1 month 97%
  3 months 91%
  6 months 85%
- **LIFE EXPECTANCY:**
  STANDBY USE 3 to 5 years
  CYCLE USE (approx.):
  100% depth of discharge 250 cycles
  50% depth of discharge 550 cycles
  30% depth of discharge 1200 cycles
- **SEALED CONSTRUCTION:**
  Can be operated in any position without leakage.
- **STANDARD TERMINAL**
  Quick Disconnect .250
- **HOUSING MATERIAL:**
  ABS Resin
- **OPTIONAL:**
  Container and cover made from Flame Retardant ABS (UL94-V0/L.O.I.>28%)

Figure 25. Genesis NP12–12 rechargeable lead-acid battery specifications.

The battery power rating was calculated from average current and average voltage off of the specification sheet. The battery specification sheet in Figure 25 shows a linear relationship between the power draw time and amp-hour rating between across the five, 10, and 20-hour draw times under “nominal capacity.” Interpolation for a draw time of six hours gave a battery capacity of 10.6 Ah. Dividing 10.6 Ah by six hours yields an average battery current of 1.78 A.

The battery voltage at the end of discharge between the five and 10-hour draw times, under the “nominal capacity” heading in Figure 25, is 10.2 and 10.5 volts, respectively. For a six hour draw period, linear interpolation between the five and 10-hour draw times gives a discharged battery voltage of 10.26 V. Battery voltage as a function of time is shown in Figure 26 along with an annotation for the average voltage over the six hours.

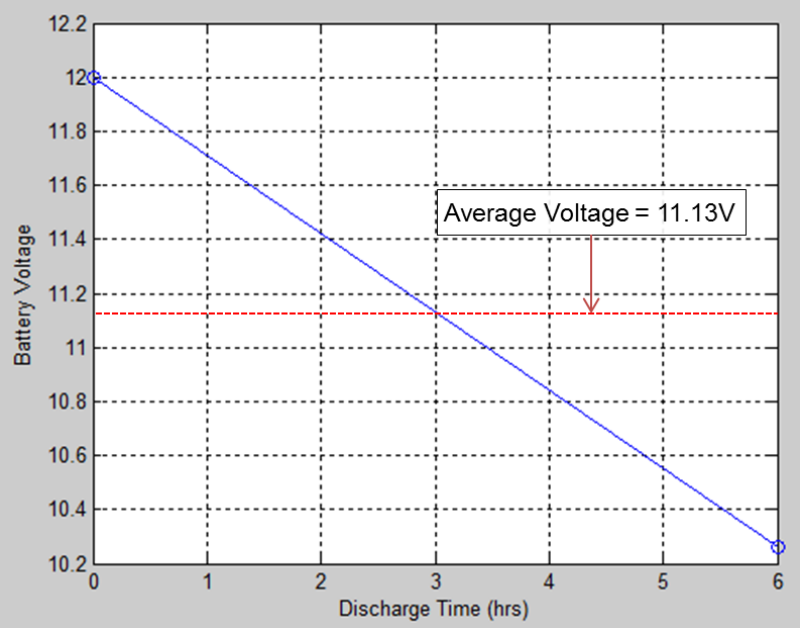

Figure 26. Battery voltage during a six hour draw period.

Next, the average battery power was calculated over the six hour time by multiplying the battery’s average voltage and average current. This resulted in a power of

(1.78 A) (11.13 V), or 19.8 W, per battery. Based on an approximate value of 20 W per battery, it was concluded that 50 batteries were required to provide 1 kW of power for six hours.

The EMS can charge the battery bank whenever a generator is connected and its capacity exceeds the load power demand. The battery specification sheet limits the battery charging current to 3 A and the charging voltage to 15 V for a maximum of charging power of 45 W per battery. Therefore, for 50 batteries the maximum allowable charging power is 2.35 kW. The 50 batteries necessary to provide 1 kW for six hours weigh a total of 441 pounds and occupy a space 3 feet wide by 3.5 feet long by 6 inches tall. At approximately $25 per battery, the total cost for the batteries is $1,250.

E. CHAPTER SUMMARY

Traditional employment of two generators and their associated loads was compared to a microgrid architecture built around the EMS. Four principles guide EMS logic design, the most vital being the EMS's requirement to provide uninterrupted power to critical loads. EMS power source selection decisions are based upon system states such as load demand, generator capacity, and battery bank SoC. A simple RC circuit was used to illustrate the chosen method of power calculation used in the EMS model. Various battery technologies were introduced, and the lead-acid battery was used ultimately chosen to form the basis of the EMS battery bank. Size, weight, and cost were estimated for a lead-acid battery bank capable of providing 1 kW for six hours.

IV. SAMPLE SCENARIO USED TO APPLY EMS FUNCTIONALITY

A. INTRODUCTION

In this chapter overall generator fuel consumption was compared for two different power architectures. The loads remained the same in the two architectures and included small appliances such as laptop computers, overhead light-emitting diode (LED) lighting, radios, and battery chargers as well as higher power appliances like a refrigerator, an ECU, and a microwave oven. A simple power architecture was chosen consisting of two generators and their respective loads and then compared to optimized an architecture using an EMS.

B. TWO POWER ARCHITECTURES

The generators are assumed to be single-phase, 120 V_{rms}, 60 Hz, diesel powered synchronous machines. In the traditional architecture, the two generators provided power for two distinct sets of loads independent from one another. We estimated a combined peak power demand 4 kW for the small appliances connected to smaller generator based upon load data from [3]. The larger generator was responsible for powering larger loads such as an air conditioner and refrigerators with a peak power demand of 16 kW.

The next decision regards the size of the generators needed for our control case. One method of determining generator capacity is by calculating the sum of the peak power requirements of all connected loads and choosing a generator slightly larger as to ensure an excess power margin. In the military, utilities Marines typically select a generator such that the sum of all connected loads at peak power represents only 80 percent of the generator's capacity [11], a paradigm we called the 80-percent rule. Using the 80-percent rule as our guide for the traditional scenario, we selected a 5 kW capacity for Generator 1 and a 20 kW capacity for Generator 2. The layout of the two generators and their respective loads is shown in Figure 27.

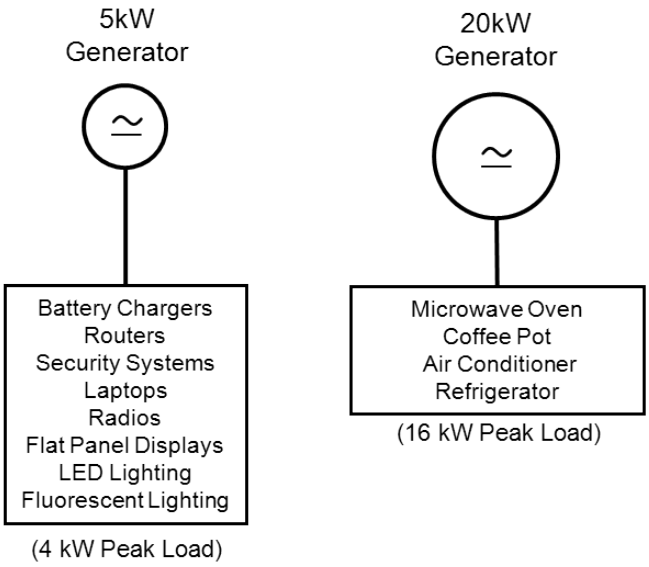

Figure 27. Generators and loads used in the traditional scenario.

The second architecture used the EMS to interface between the generators, loads, and a battery bank. The block diagram of the EMS-based architecture is shown in Figure 28.

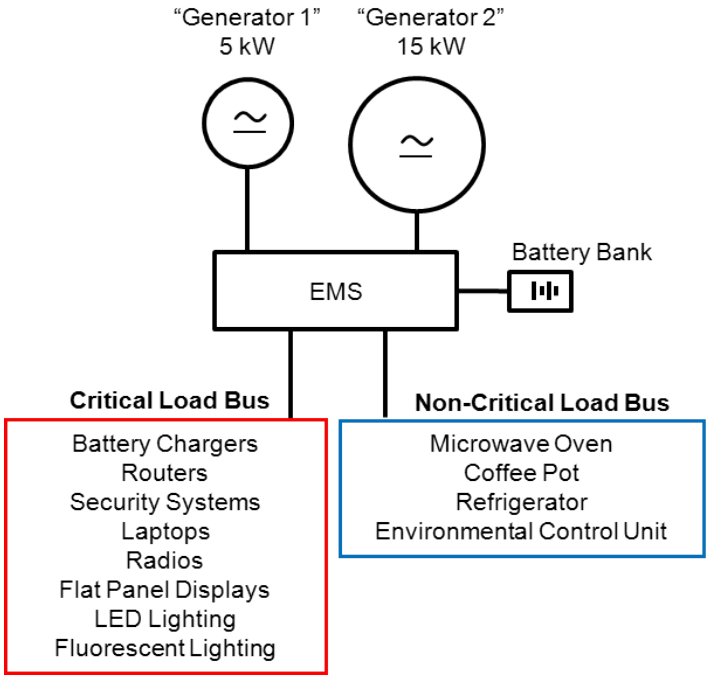

Figure 28. Generators and loads connected by the EMS.

It is important to note that for our EMS-based scenario, we replaced the 20 kW generator from Figure 27 with a 15 kW generator in Figure 28. We chose a smaller generator for two reasons. First, under the traditional scenario the intent behind limiting generator output by 20 percent of its total capacity is to create a safety margin for transient conditions that may place additional demand upon the generator. However, modern generators such as those employed by the Marine Corps are designed to handle sustained operation at 100 percent and are capable of "absorbing transient loads above their rated load without harm to the system" [11]. Reviewing the trend between generator loading and efficiency in Figure 2 reveals that limiting generator loading to 80 percent results in sub-optimal generator efficiency. Furthermore, under-utilizing a generator for extended periods of time results in a higher probability of failure when the load is increased [11]. Therefore the 80 percent maximum loading constraint imposes an unnecessary cost in terms of limited fuel efficiency and increased maintenance.

Second, the EMS enabled us to use a smaller generator because it offered the use of batteries to supply additional power or shed the non-critical loads during transient peak power situations. A tradeoff existed between how much power we could supplement with batteries and how heavy and expensive the bank of batteries would be. We chose a battery pack consisting of 150 Genesis NP12–12 lead acid batteries. This battery pack weighs roughly 1,200 pounds and measures 3 feet wide by 3.5 feet long by 1.5 feet tall. Compared to the traditional scenario, the added weight of the battery pack is partially offset by 550 pounds, which is the difference between the 15 kW and 20 kW generators. At full charge this battery pack is capable of providing 3 kW for six hours.

While we intend to use the battery pack as a primary power source during long periods of low load demand, the battery bank is also capable of providing much higher power. For example, at full charge each individual battery can sustain a one hour draw rate shown of 7.2 A, as shown in Figure 25. The average voltage over a one hour period, as the batteries discharge from 12 V down to 9.6 V, is 10.8 V. Therefore, each battery can provide (7.2 A) (10.8 V) = 77.8 W. Using 150 batteries our battery pack can provide

(150) (77.8 W) = 11.7 kW for one hour. Even higher power draw is possible for shorter discharge durations since the maximum sustained current per battery is 40 A, and the maximum short duration current is 360 A.

C. NOTIONAL 24-HOUR LOAD PROFILE

Based on sampled load data from that is shown in Figure 29. This notional load profile is just one of many scenarios that could be applied to the EMS and is useful in illustrating room for optimization under traditional generator employment.

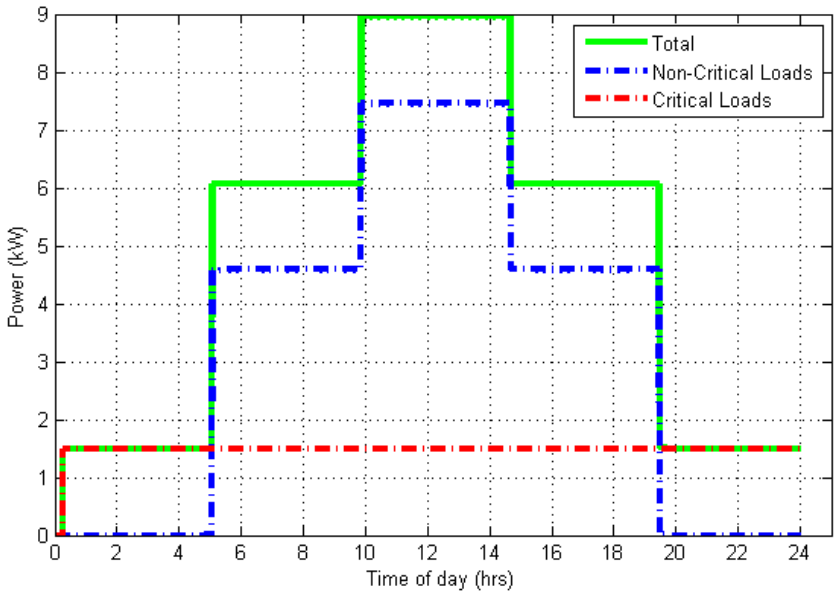

Figure 29. Notional 24-hour load demand profile.

The critical loads in this scenario are the lower power loads, which are connected to the smaller generator in the traditional scenario shown in Figure 27, or to the critical load bus if using an EMS. In the sample scenario we assumed the critical loads remain relatively constant throughout the day, reflected by the dashed red line in Figure 29. The blue dashed line represents the power demanded by the non-critical loads. As shown in Figure 27, the non-critical loads in this scenario are connected to the larger generator, or if using the EMS, they are connected to the non-critical bus. The sum of the critical and non-critical loads is the total load demand and is shown by a solid green line.

Throughout the day the total load demand ranges from 1.5 kW at night up to 9 kW during the afternoon. The total load demand is greatest during the afternoon, which correlates to the warmest time of the day when air-conditioners and ECUs are most often running.

We assumed that under the traditional generator employment both generators run around-the-clock. We considered this method of employment as our control case to which we compare the EMS-enabled microgrid later in Chapter V. Based on the logic presented in Chapter III, we programmed our Simulink model EMS to make power source selection decisions. The model, along with its initial conditions file, is contained in Appendix A and B. The power source selection decisions depended upon very few user inputs that consisted of the maximum power rating of each connected generator and maximum desired power that the EMS may draw from the battery pack. To test the EMS logic, we condensed the 24-hour load profile from Figure 29 and into a 1.5 second version shown in Figure 30.

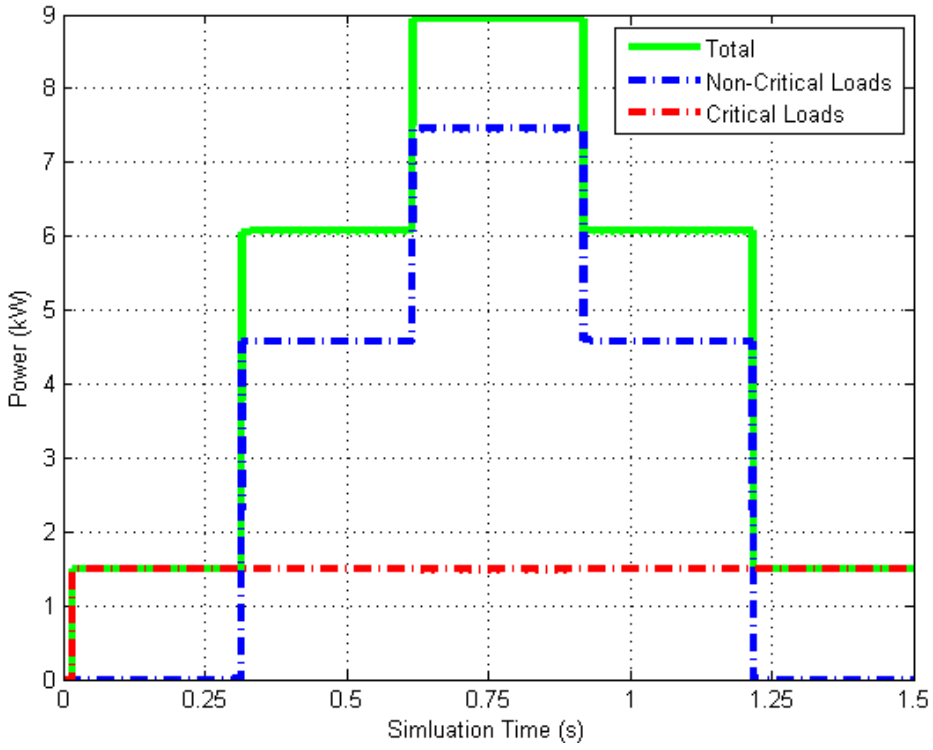

Figure 30. Twenty-four hour load demand profile from Figure 29 condensed to a 1.5 second version for use simulation.

Using a series of steps, we simulated different sized resistive loads switching on and off according to the power steps presented in the load profile. Applying the desired load profile from Figure 30 to the EMS model yielded the actual load profile in Figure 31. The step events from Figure 30 are identified in Figure 31 as well as the maximum power thresholds used by the EMS logic for the battery pack, Generator 1, and Generator 2.

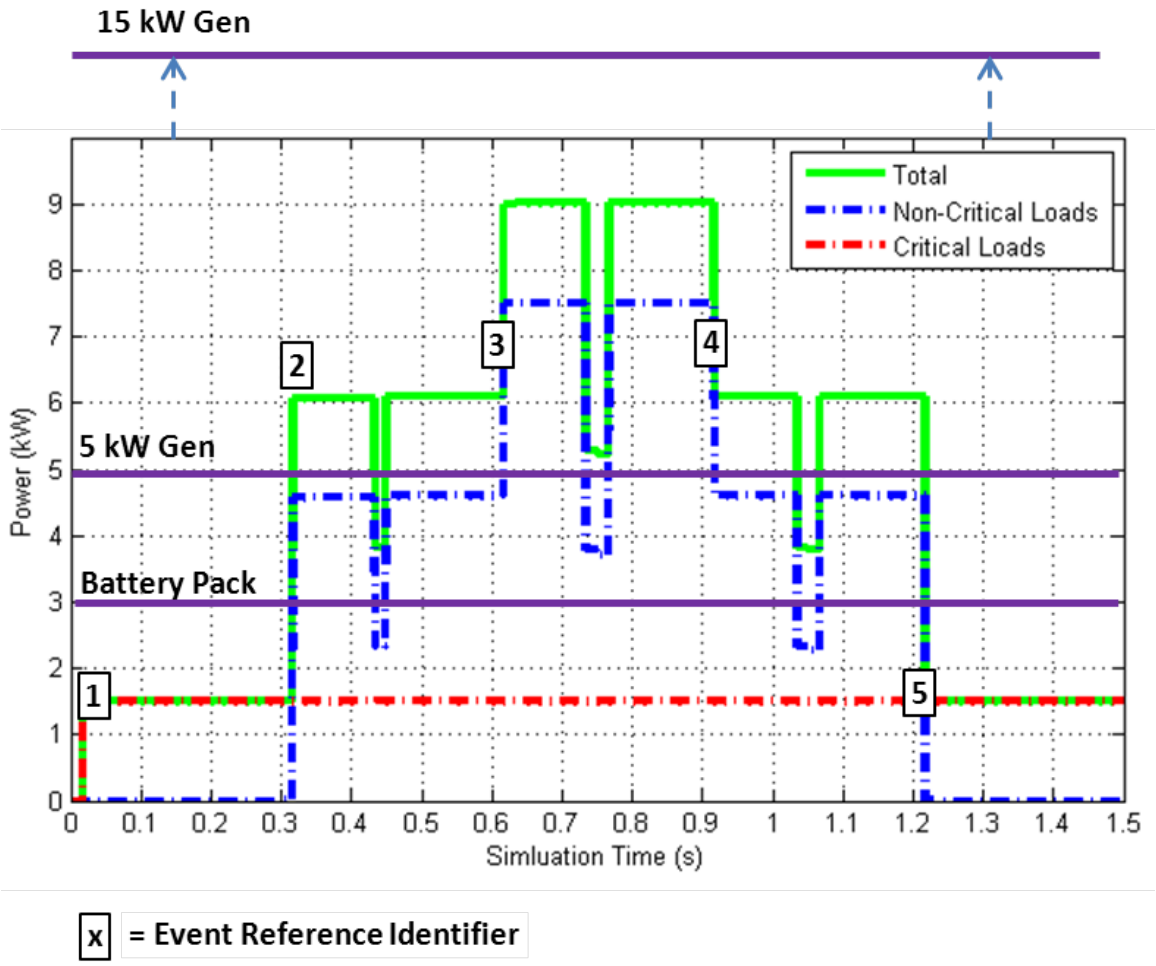

Figure 31. Load profile produced by the simulation, using the desired loads in Figure 30.

Important system states are shown in Figure 32 corresponding to the power profile and event numbers shown in Figure 31.

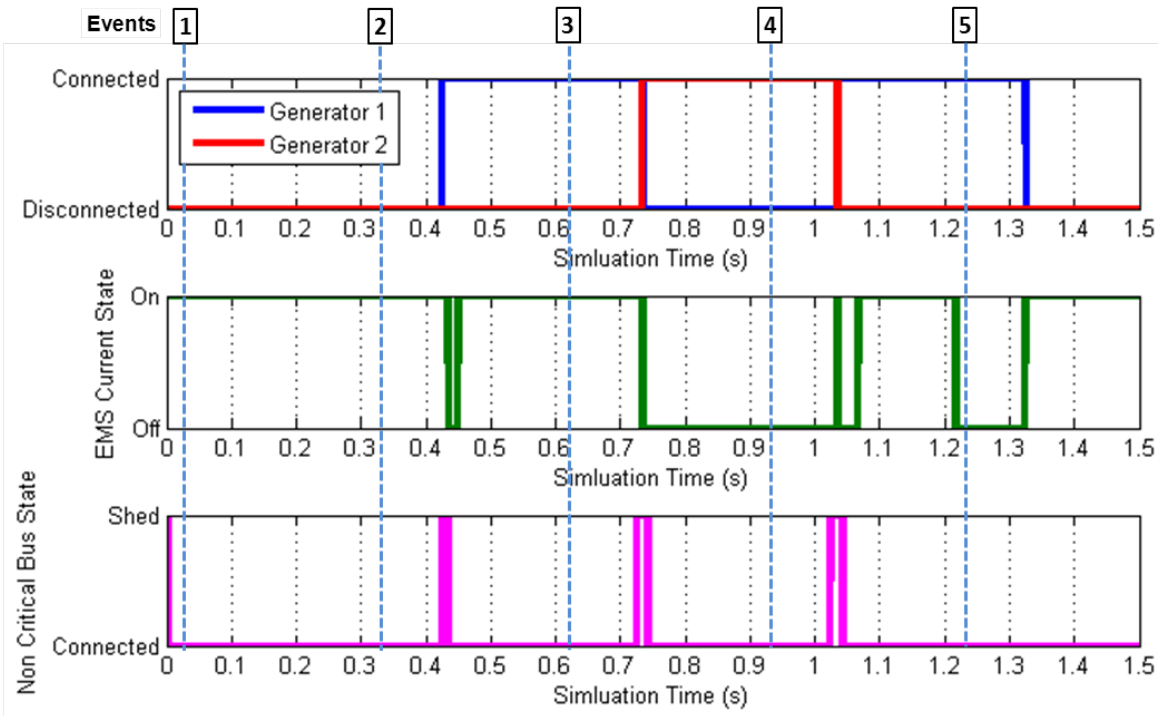

Figure 32. EMS states according to the events identified in Figure 31.

Event 1 corresponds to the initial startup of the system. Only the critical loads are energized at the beginning of the simulation, accounting for a constant 1.5 kW power demand as shown in Figure 31. Since the 1.5 kW load is within our designed maximum continuous battery power of 3 kW, the EMS uses the battery as the only source of power to the loads. Accordingly, both Generator 1 and Generator 2 remain disconnected and the EMS acts a voltage source and supplies current to the load as seen in the top and center plots in Figure 32, respectively.

The first step increase in total load power occurs at Event 2 in Figure 31 and corresponds to non-critical loads switching on and drawing 4.6 kW of power. The sum of the constant 1.5 kW critical loads and the 4.6 kW demand of the non-critical loads during this time yields a total power of 6.1 kW. At Event 2, the total load demand of 6.1 kW exceeds the 3 kW battery limitation. However, the EMS does not immediately take corrective action, as evidenced by the unchanged states at Event 2 in Figure 32. We implemented a timer to prevent the EMS from taking a corrective action unless a power threshold remains exceeded for at least 0.10 seconds. The reason we implemented such a

delay is to prevent transient power spikes from altering the operational state of the EMS. Therefore, after 0.10 seconds have elapsed following Event 2, wherein the load power continues to exceed the battery's desired 3 kW limit, the EMS initiates a handoff from the battery pack to a Generator 1. The EMS selects Generator 1 as the desired generator, vice Generator 2, because the design goals we outlined in Chapter III state that the EMS should always choose the smallest generator possible to power the load. The combination of Generator 1's 5 kW capacity, plus the additional battery capacity of 3 kW, is sufficient to power the 6.1 kW sensed load.

In a hardware implementation of the EMS, a handoff from the battery pack or a generator to another generator begins with the EMS sending a startup signal to desired generator. Once the desired generator is operational the EMS continues with the first step of the handoff we modeled, shedding the non-critical load bus.

The handoff decision resulting from Event 2 triggers the EMS to shed the non-critical load bus. However, the EMS only sheds the non-critical load temporarily, and the EMS restores it as soon as it connects Generator 1. After EMS sheds the non-critical bus, it continues to operate in island mode until Generator 1's voltage is in phase with the output bus and at a zero-voltage crossing. At the zero-crossing the EMS connects Generator 1 using a thyristor. In our model, we assumed both generators were always running and in-phase with the output bus voltage in order to minimize the duration of the simulation.

The shed event is evident by a dip in non-critical load power and the corresponding total load demand following Event 2 in Figure 31. In a real-life scenario the shed event is important because it may take significant time before Generator 1 is turned on, fully operational, in phase with the output bus voltage, and connected to the EMS. The non-critical bus shed prevents the batteries from supplying a greater power level than intended during this time. Since our model used in-phase and always-on voltage sources for generators, the period of time between generator handoffs spans only 16.7 ms, equal one period of the 60 Hz voltage waveform. The EMS's power calculation never reaches steady-state and, therefore, is inaccurate during load-shedding between

power source hand-offs. However, the total power does significantly decrease following Event 2 in Figure 31, and had the hand-off event taken even one cycle longer, the total power measurement would reflect the correct 1.5 kW value.

Once the EMS connects Generator 1, the total load is 1.5 kW since the non-critical bus is shed, which is within the capacity of Generator 1 alone. Hence, the EMS stops supplying current to the load. This occurs just after 0.4 seconds as seen by the momentary transition from EMS current “on” to “off” in the bottom plot in Figure 32 . After a short delay resulting from turning the non-critical load bus thyristor on, the total load returns to 6.1 kW. In this state the EMS draws 1.1 kW from the battery pack to maintain Generator 1 at 100 percent capacity.

Another load step increase occurs at Event 3 in Figure 31 as a result of an increased non-critical load demand. The non-critical load steps from 4.6 kW to 7.5 kW, causing the total load to increase from 6.1 kW to 9 kW. A total load of 9 kW is greater than the 8 kW of power available, which takes into account 5 kW from Generator 1 and a maximum of 3 kW from the battery pack. The over-power condition remains for longer than 0.1 seconds and thus triggers the EMS to take corrective action. The EMS initiates a handoff from the 5 kW generator to the 15 kW generator by first shedding the non-critical load bus. The load shed signal is apparent as the bottom plot goes high at approximately 0.72 seconds in Figure 32. Concurrently, the total load demand decreases toward 1.5 kW in Figure 31 since the non-critical loads are disconnected. Approximately 16.7 ms after the EMS disconnects Generator 1 it connects to Generator 2. After Generator 2 is connected the EMS stops supplementing current because Generator 2 has 15 kW of capacity and the load is only 1.5 kW. The EMS current turn-off event is shown by the middle plot going low after Event 3 in Figure 32. With Generator 2 connected, the EMS connects the non-critical bus, and the total load returns to 9 kW. Generator 2 has 6 kW of excess capacity since it serves a 9 kW load but has 15 kW of capacity. In this situation, the excess capacity can be used to recharge the battery pack.

The non-critical load demand drops from 7.5 kW to 4.6 kW at Event 4 in Figure 32. As a result the total load decreases from 9 kW to 6.1 kW. After 0.1 seconds at the total power level of 6.1 kW, the EMS initiates a handoff from the larger generator to the

smaller generator. As with previous handoffs the EMS first sheds the non-critical bus, shown in the bottom plot stepping from “connected” to “disconnected” just after 1 second in Figure 32. With the non-critical bus shed the EMS disconnects Generator 1 and enters island mode, evident by the EMS current changing from “off” to “on” in Figure 32. Next, the EMS connects Generator 1. With Generator 1 connected the EMS turns off the current source since the load is 1.5 kW and Generator 1 has 5 kW capacity. Next, the EMS re-connects the non-critical load bus, and the total power increases from 1.5 kW to 6.1 kW in Figure 31. After 0.1 seconds at a 6.1 kW of load demand the EMS supplies 1.1 kW of supplemental current in order to maintain Generator 1 at 5 kW of loading.

Finally, at Event 5 all of the non-critical loads turn off and the total load demand reduces to just the 1.5 kW critical load. After 0.1 seconds at 1.5 kW the EMS’s logic dictates a handoff from Generator 1 to the battery pack. With Generator 1 disconnected, the EMS enters island mode and supplies the load current as seen at 1.33 seconds in middle plot of Figure 32. If the EMS sensed the battery state of charge was lower than a defined threshold value it would instead remain connected to Generator 1 and use the excess power capacity to recharge the battery bank.

In summary, the model demonstrated that through varying modes of operation the EMS continuously provided critical load power. The only case not covered in this simulation is the scenario where the total power demand exceeds that of the 15 kW generator and 3 kW of supplemental EMS current drawn from the battery pack. If this happens the EMS must shed the non-critical bus until the total load demand decreases below 18 kW. However, based on trends from [3] it is unlikely that all of the connected loads will operate simultaneously at their peak power requirements.

D. CHAPTER SUMMARY

An example scenario to the two power architectures introduced in Section A of Chapter III was applied in this chapter. The scenario included two sets of loads, their respective peak power requirements, and a notional power profile over a 24-hour period. Generator sizes used in the traditional method of generator employment were based up on 80 percent of the total peak load to which they were connected. The EMS-enabled

architecture took into account the battery bank's capability to supplement generator power in order to enable the use of a 15 kW generator in place of a 20 kW generator. The 24-hour load profile was condensed into 1.5 seconds and used in a simulation that modeled EMS's operation. A detailed analysis of EMS states showed that the EMS was able to continuously power the critical loads while receiving power from the smallest capable generator or entirely from the battery bank as appropriate.

THIS PAGE INTENTIONALLY LEFT BLANK

V. RESULTS AND CONCLUSION

A. RESULTS

The goal of this thesis was to demonstrate how an EMS-enabled microgrid saves fuel as compared to the traditional method of generator employment. The total fuel consumed by generators using the traditional method and the EMS-enabled method of generator employment are compared in this chapter. For the traditional scenario, the 24-hour power profile from Figure 29 was applied to the generator setup shown in Figure 27. We chose a 5 kW generator and a 15 kW generator for the EMS-enabled architecture with the critical and non-critical loads connected to the EMS as shown in Figure 28.

We used fuel flow data from [13] and [14] to estimate fuel flow equations for the 5 kW, 15 kW and 20 kW generators with respect to their operating points. The plot of each generator's estimated fuel flow in gallons per hour (gph) as a function of its operating point is shown in Figure 33.

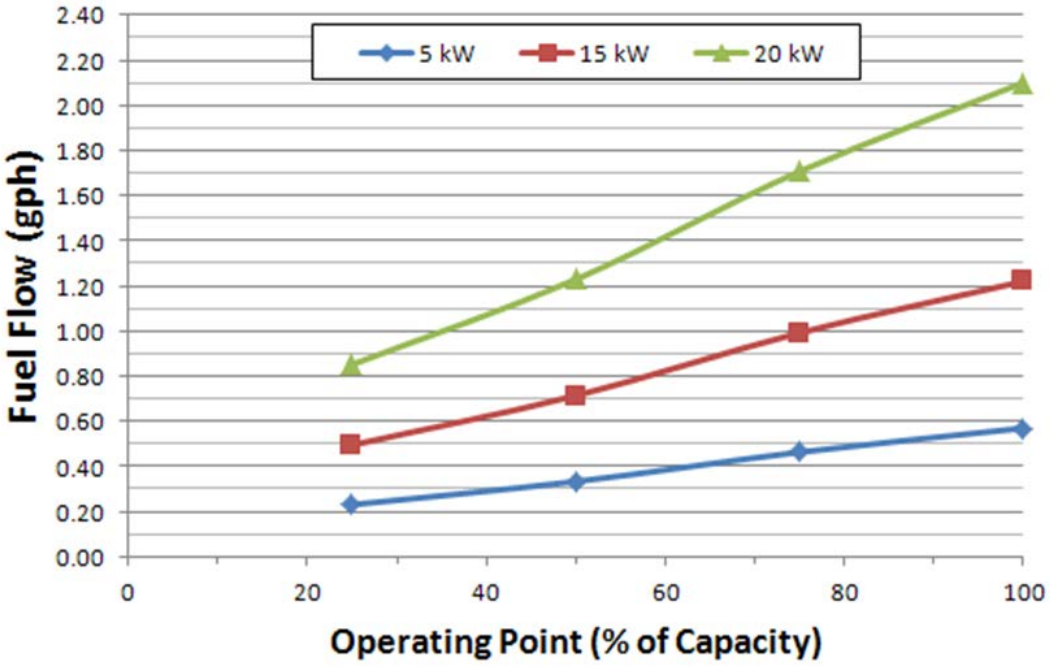

Figure 33. Plots of estimated fuel flow curves for the 5 kW, 15 kW and 20 kW diesel generator. After [13] and [14].

Best-fit, first-order equations for the fuel flow plots from Figure 33 are presented in Table 1. Each generator in the first column has a corresponding fuel rate *f(x)* measured in gallons per hour (gph) on the same row. The subscript applied to *f(x)* corresponds to the rating of the generator to which the equation applies, and the variable *x* is the operating point of the generator expressed as a percentage value from 0 to 100.

Table 1. Generator fuel flow equations.

Generator Size	Fuel Flow (gph)
5 kW	$f_5(x) = 0.0046x + 0.113$
15 kW	$f_{15}(x) = 0.0098x + 0.2419$
20 kW	$f_{20}(x) = 0.0169x + 0.4163$

Each generator's loading as result of traditional generator employment is shown throughout the 24-hour profile in Figure 34. We calculated respective generator fuel flow at each power level using the corresponding fuel flow equation in Table 1. Multiplying each generator's fuel flow by the duration of time at that rate gave us the fuel consumed for that period. These steps as well as the total fuel consumed in the 24-hour period using traditional generator employment are shown in Table 2.

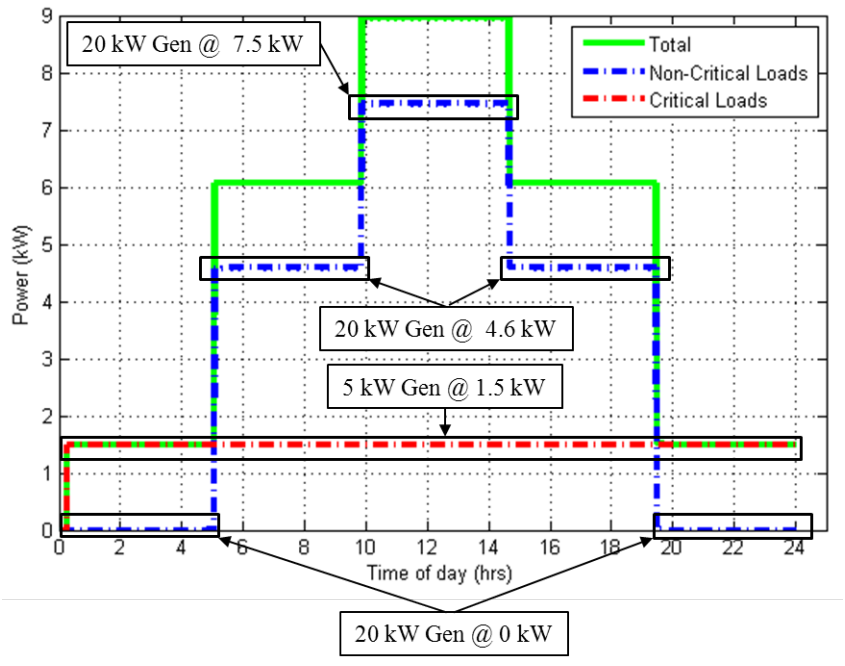

Figure 34. Generator loading using traditional generator employment.

Table 2. Twenty-four hour fuel consumption using traditional generator employment.

Power Source	Time of Day	Duration (hrs)	Generator Load (kW)	Generator Operating Point	Fuel Flow (gph)	Fuel Consumed (gal)
5 kW Gen	0000-2359	24	1.5	30.0%	0.251	6.024
20 kW Gen	0000-0500	5	0	0.0%	0.4163	2.0815
	0500-1000	5	4.6	23.0%	0.805	4.025
	1000-1430	4.5	7.5	37.5%	1.05	4.725
	1430-1930	5	4.6	23.0%	0.805	4.025
	1930-2359	4.5	0	0.0%	0.4163	1.87335
					TOTAL:	**22.75385**

Determining the generator loading for the EMS-enabled method of generator employment required additional calculations as compared to the traditional method because the battery pack's state of charge factors into EMS power source selection logic. We maintained a tally of the battery pack's state of charge throughout the 24-hour scenario from Figure 29. The battery bank's total energy storage capacity is given by

$$E_{total} = P_0 t_0 , \tag{9}$$

where E_{total} is the battery pack's total useable energy in Joules, P_0 is the sustained power the EMS may draw from the battery pack in Watts, and t_0 is the duration in seconds over which P_0 is drawn. The amount of energy drawn from the battery pack is given by

$$E_{drawn} = P_{draw} t_{drawn} , \tag{10}$$

where E_{drawn} is the energy drawn in Joules, P_{draw} is the amount of power the batteries are providing in Watts, and t_{drawn} is the duration of time in seconds over which P_{draw} is sustained. The difference between E_{total} and the sum of E_{drawn} for varying power levels gives the energy remaining in the battery pack $E_{remaining}$. The battery bank's state of charge is expressed as a percentage given by

$$SoC = \frac{E_{remaining}}{E_{total}} 100\% . \tag{11}$$

The Simulink model used in Chapter IV did not track the battery bank state of charge since the scenario lasted only 1.5 seconds. However, in the 24-hour scenario it was important that we tracked the state of charge, which we did manually. First, we

calculated the battery pack's total energy storage capacity E_{total} using Equation 9 where P_0 was 3 kW and t_0 was 6 hours, which resulted in E_{total}=64.8 MJ. EMS logic remained the same as in Chapter IV with one exception. If the EMS sensed a situation where a connected generator had a power capacity greater than the load demand, it would first charge the batteries up to 100 percent SoC before handing off to a smaller power source.

The EMS logic from Chapter IV combined with the battery bank state of charge tracking resulted in the load profile shown in Figure 35. Boxed regions define different EMS generator and battery modes. It is important to note that while load shedding does indeed occur between generator handoffs, it is not depicted due to the short amount of time it takes to handoff generators relative to the 24-hour time scale.

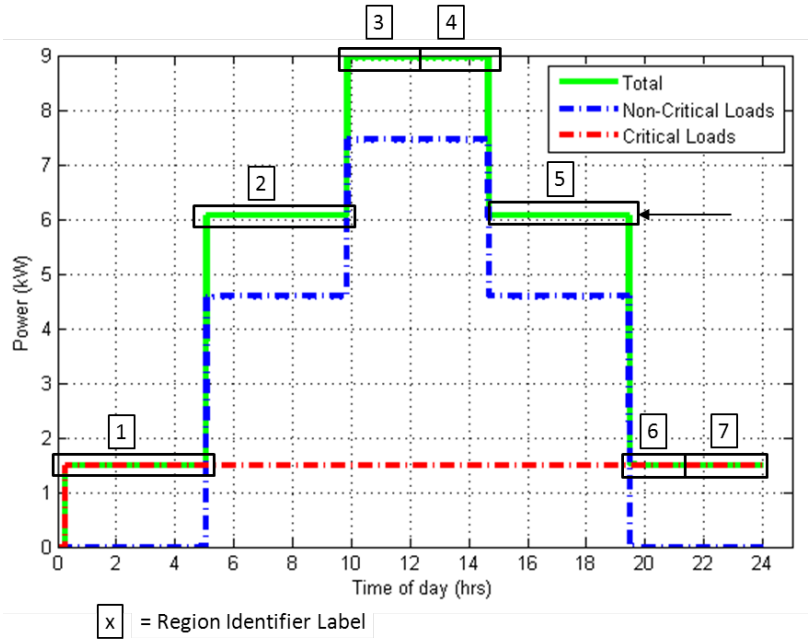

Figure 35. Twenty-four hour profile using EMS-enabled generator employment.

The regions identified in Figure 35 correspond to information contained in the rows in Tables 3 through 5. A summary of which generator the EMS selected, the battery bank's mode of operation, and the battery bank's SoC is shown in Table 3. More detailed

data concerning our calculation of the battery bank's SoC is shown in Table 4. The total fuel consumption resulting from using the EMS-enabled architecture to supply power to the 24-hour load profile is tabulated in Table 5.

Table 3. EMS operational states corresponding to regions identified in Figure 35.

Region	Time of Day	Load Demand (kW)	Generator Selected	Generator Load (kW)	Battery Mode	Battery Load (kW)	Initial SoC	Final SoC
1	0000-0500	1.5	NONE	0	Supply	1.5	100.0%	58.3%
2	0500-1000	6.1	5 kW	5	Supply	1.1	58.3%	27.8%
3	1000-1210	9	15 kW	15	Charge	-6	27.8%	100.0%
4	1210-1430	9	15 kW	9	Off	0	100.0%	100.0%
5	1430-1930	6.1	5 kW	5	Supply	1.1	100.0%	69.4%
6	1930-2105	1.5	5 kW	5	Charge	-3.5	69.4%	100.0%
7	2105-2359	1.5	NONE	0	Supply	1.5	100.0%	75.6%

Table 4. Battery bank SoC corresponding to regions identified in Figure 35.

Region	Duration (hrs)	Battery Load (kW)	Intial Capacity (MJ)	Energy Drawn (MJ)	Remaining Capacity (MJ)	Initial SoC	Final SoC
1	5	1.5	64.8	27.0	37.8	100.0%	58.3%
2	5	1.1	37.8	19.8	18.0	58.3%	27.8%
3	2.17	-6	18	-46.8	64.8	27.8%	100.0%
4	2.33	0	64.8	0.0	64.8	100.0%	100.0%
5	5	1.1	64.8	19.8	45	100.0%	69.4%
6	1.57	-3.5	45	-19.8	64.8	69.4%	100.0%
7	2.92	1.5	64.8	15.8	49.0	100.0%	75.6%

Table 5. Twenty-four hour fuel consumption using the EMS-enabled generator employment.

Region	Selected Generator	Duration (hrs)	Generator Load (kW)	Generator Operating Point	Fuel Flow (gph)	Fuel Consumed (gal)
1	NONE					
2	5 kW	5	5	100%	0.573	2.865
3	15 kW	2.17	15	100%	1.23	2.6691
4	15 kW	2.33	9	60%	0.83	1.9339
5	5 kW	5	5	100%	0.573	2.865
6	5 kW	1.57	5	100%	0.573	0.89961
7	NONE					
					TOTAL:	**11.23261**

Comparing the total fuel consumption by the generators used in the traditional scenario to those used in the EMS-enabled scenario validates this thesis. The EMS managed the available power sources such that the load demand was met using a total of 11.23 gallons of fuel over the 24-hour period. In contrast, the traditional method of generator employment resulted in the generators consuming 22.75 gallons of fuel. The EMS enabled a fuel savings of 50.6 percent over the traditional scenario.

B. CONCLUSION

We made many educated presumptions in the conduct of this thesis in order to overcome information gaps and move forward with the research. These ranged from the load profile used in our scenario to the generators' fuel flow rates with respect to loading. In addition our modeling assumed certain ideal factors such as lossless power electronics and perfectly sinusoidal voltage sources, which do not exist in real life. However, the purpose of this thesis was to explore the concept of employing generators in a more efficient manner. To this end we compared our two scenarios fairly using the same assumptions for both scenarios where a decision had to be made.

The 24-hour load profile we used in this thesis might seem unrealistic; that is, a set of loads with a 20 kW peak requirement never reached above 9 kW in our scenario. Surprisingly, though, such under-utilization is quite common [15]. Data collected in the field shows that FOBs contain as much as 115 kW of generator capacity for total load profiles that, in reality, seldom reach above 45 kW [3]. We feel that the EMS serves a purpose in larger microgrid architectures above 20 kW as well. Excessive generation capacity drives traditional military generator employment, but in reality these generators never operate in the most efficient manner because doctrine limits them to 80 percent loading at best. As demonstrated in this thesis, the EMS enables generators to run up to 100 percent with the battery pack ensuring additional power is available when needed.

Future investigations into the role of alternative and renewable energy sources in the EMS architecture will prove enlightening as well. For example, the EMS may incorporate solar or wind power to charge the battery pack, alleviating some of that requirement from the generators.

In a grid-connected setting, the EMS can improve power quality of one's home by injecting harmonic-cancelling current. Furthermore, the EMS can allow a homeowner to draw power from the utility grid during times of the day when electricity rates are lower, at night for instance, and store energy in the batteries. Then, during the most expensive time of the day, the EMS can supplement household load demand using the energy stored in the batteries, thereby reducing the amount of electricity drawn from the grid.

THIS PAGE INTENTIONALLY LEFT BLANK

APPENDIX: SIMULINK MODEL

A. INITIAL CONDITION FILE

```
%% Simulation
useHbridge=0;

tstep=(1.666667e-5);  % Roughly 1000 samples per cycle 60Hz cycle
tstop=1.5;
if useHbridge
    tstep=tstep/10;
end

wc=2*pi*5;  % LPF used twice in series to calculate
            % RMS values for current/voltage

%% Generator 1
Gen1Rating = 5e3;
V_Gen1_rms = 120;
fGen1 = 60; % Generator 1 frequency (Hz)
Ls1=300e-6;
Rs1=0.01;

%% Generator 2
Gen2Rating = 15e3;
V_Gen2_rms = 120;
fGen2 = 60; % Generator 2 frequency (Hz)
Ls2=300e-6;
Rs2=0.01;

%% Battery Bank (For 6 hour draw period)
BattRating = 3e3;

%% Loads

% Current Slew Rate
SlewRate = 1000;

% Critical Loads
R_crit = 120^2 / 1.5e3;

% Non-critical Loads
R_step1 = 120^2 / 4.6e3;
ton_step1 = 0.3;
toff_step1 = 0.6;

R_step2 = 120^2 / 7.5e3;
ton_step2 = 0.6;
toff_step2 = 0.9;

R_step3 = 120^2 / 4.6e3;
```

```
ton_step3 = 0.9;
toff_step3 = 1.2;

%% EMS Circuit
Lems=1160e-6;
Rems=0.1;

%% EMS as Voltage Regulator
V_EMS_rms = 120;

%% EMS as Supplemental Current Source
EMS_supp_gain = .5;
Supp_current_min_thresh = 5; % Below this RMS load current EMS will not
                             % supplement any current
Supp_current_max = 10; %A_rms

%% Output Bus Capacitor
Cfil=12e-6;

%% -----H-Bridge Model-----
%EC3150 Software lab#5 - H-bridge inverter - Dr. Giovanna Oriti
%initial condition file for model ec3150_software_lab5.mdl

Kp_v=0.06;
Ki_v=5000;
sw_freq=15000;
%vo_ref=120*sqrt(2)*2/pi;
% turns=28/115;
%Rload=2000;
%Vdc=130; original in lab
Vdc=250;
%Lin=3.22e-3;  %it includes the leakage inductance of the 60Hz xfmr,
               % which is 3mH

PWM_mode=0; %A 1 is Bipolar PWM. A 0 is Unipolar PWM.
%tstep = 1e-6;
% Lfil=1160e-6;
```

B. SYSTEM AND SUBSYSTEMS

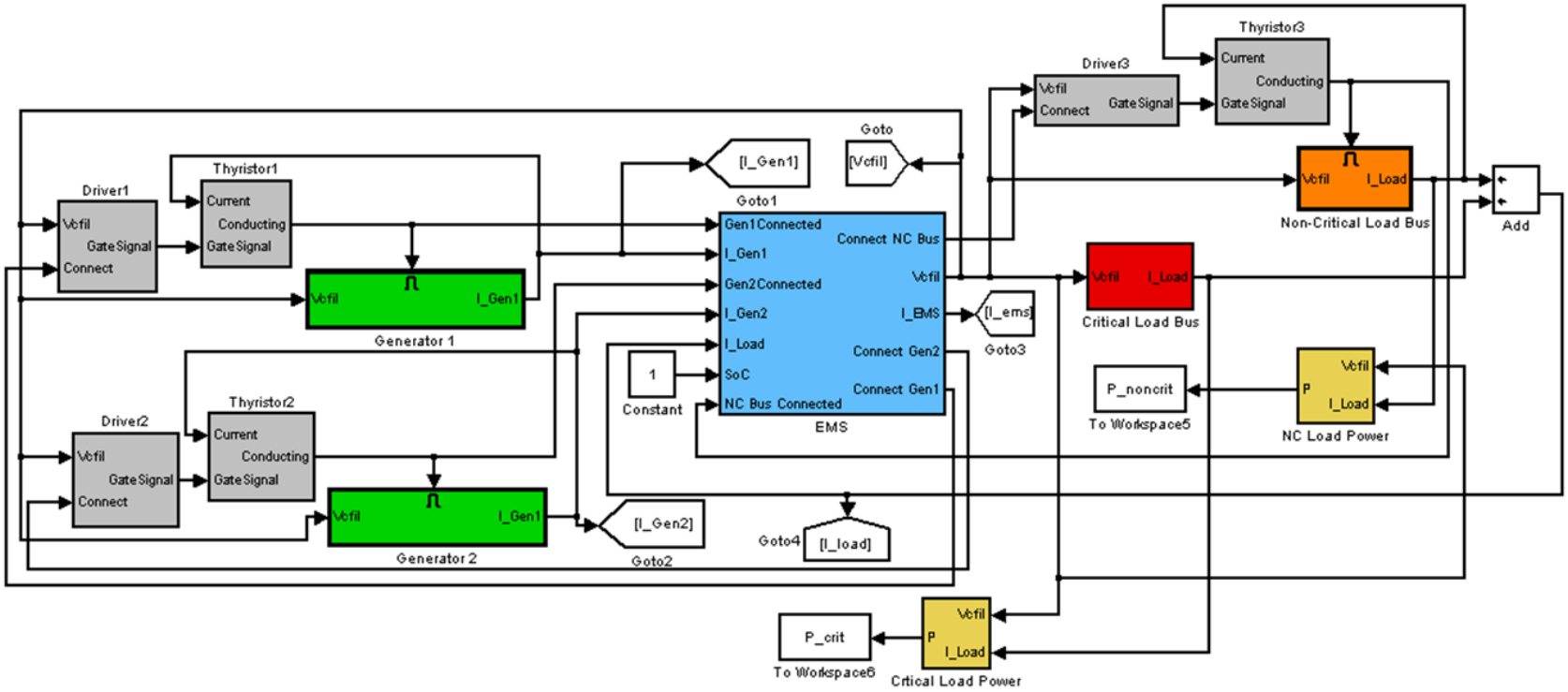

Figure 36. Model overview.

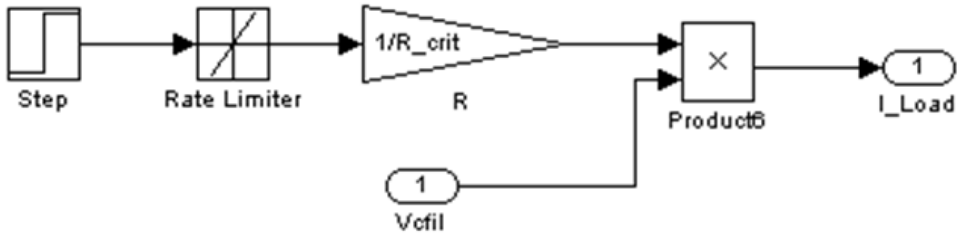

Figure 37. Critical load bus.

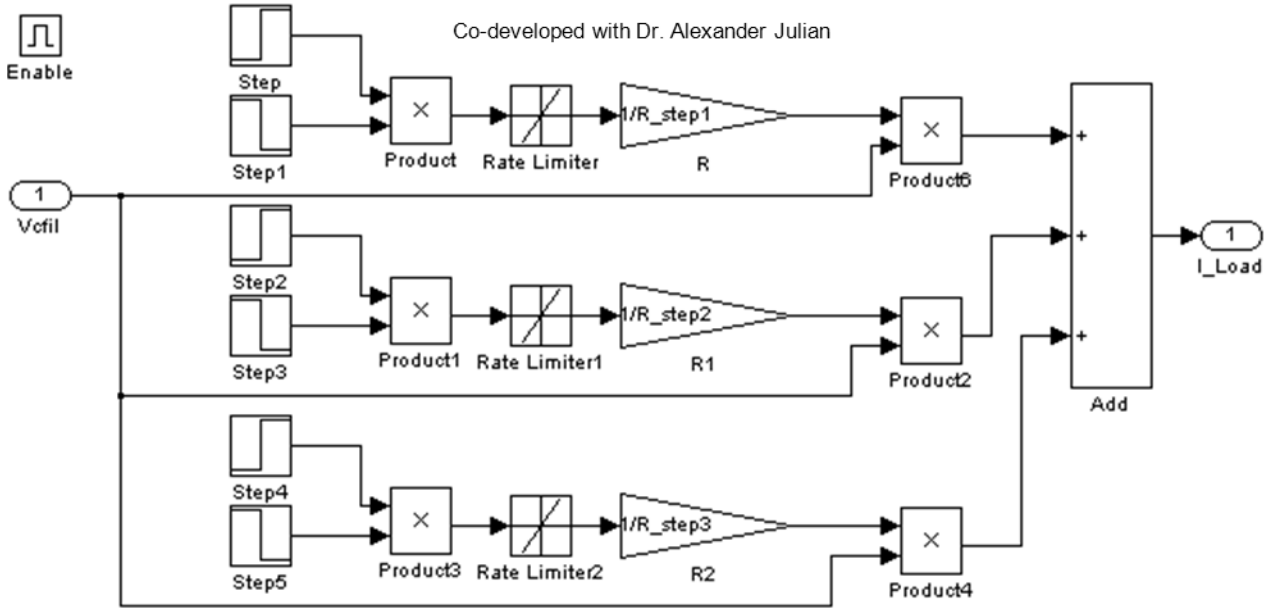

Figure 38. Non-critical load bus.

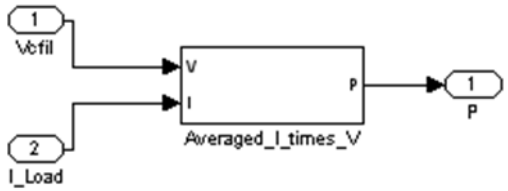

Figure 39. Power meter

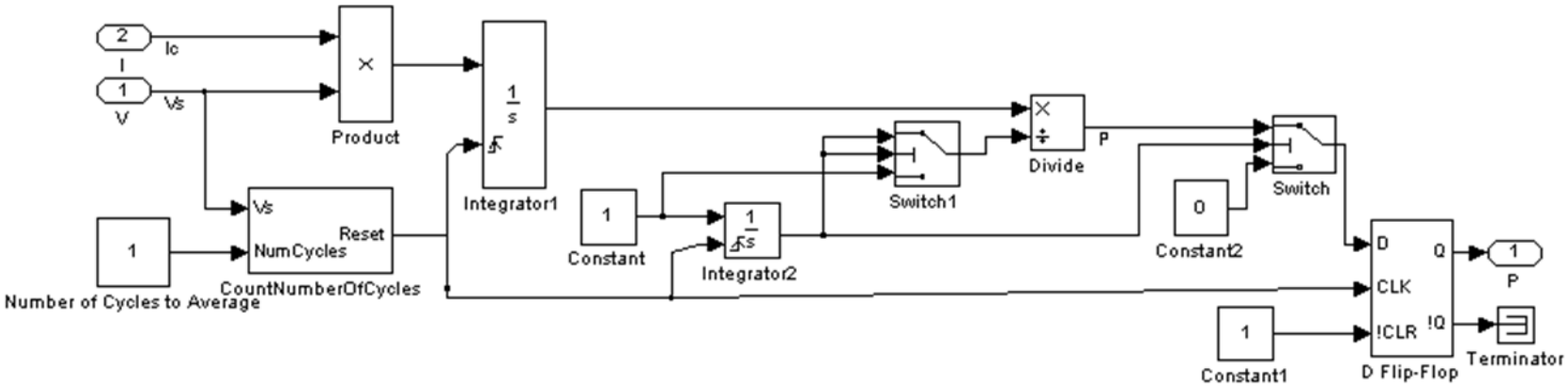

Figure 40. Power meter -> averaged_I_times_V.

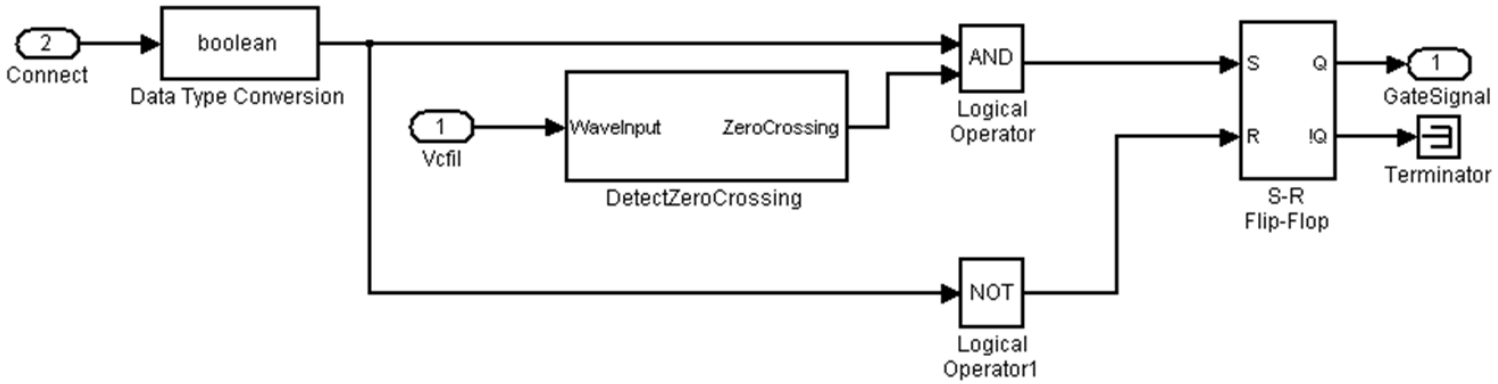

Figure 41. Thyristor driver.

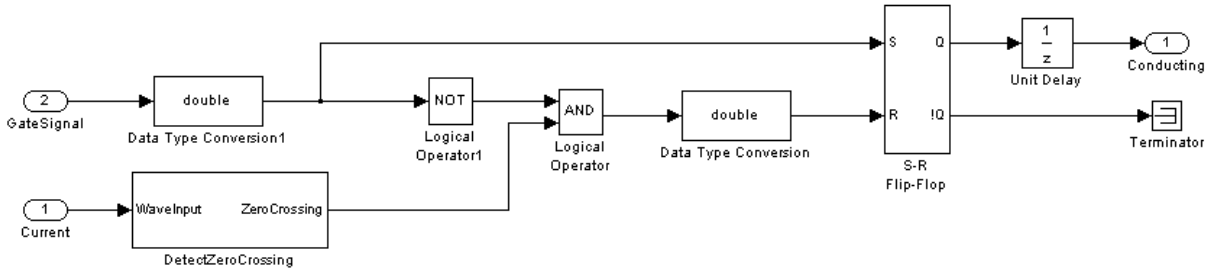

Figure 42. Thyristor.

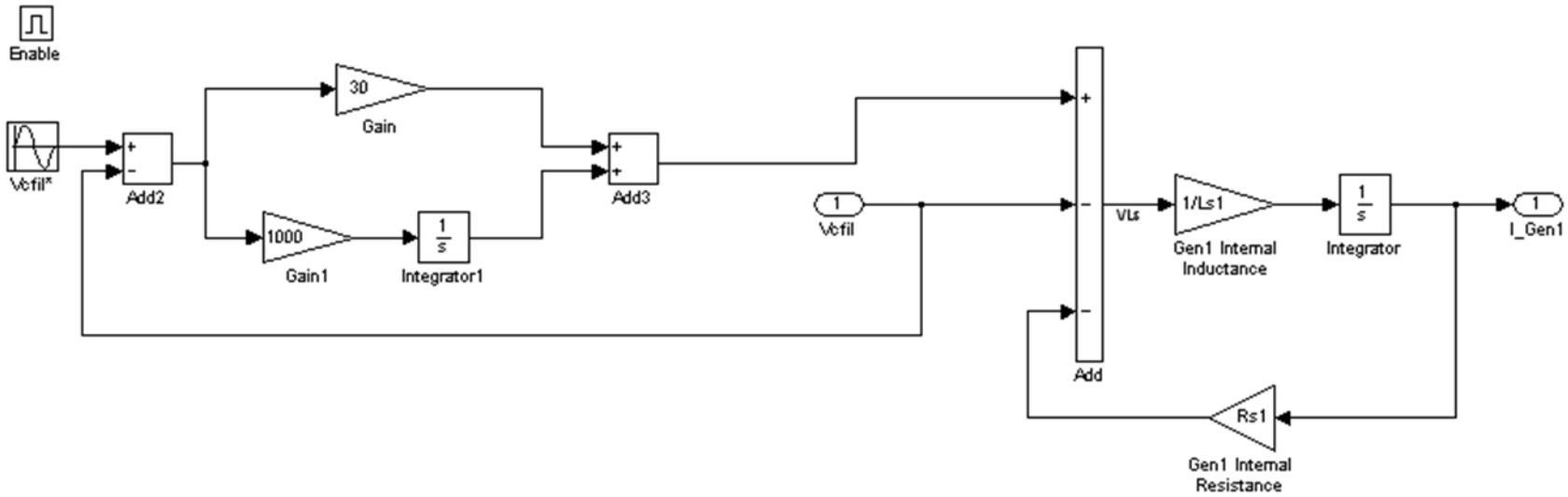

Figure 43. Generator.

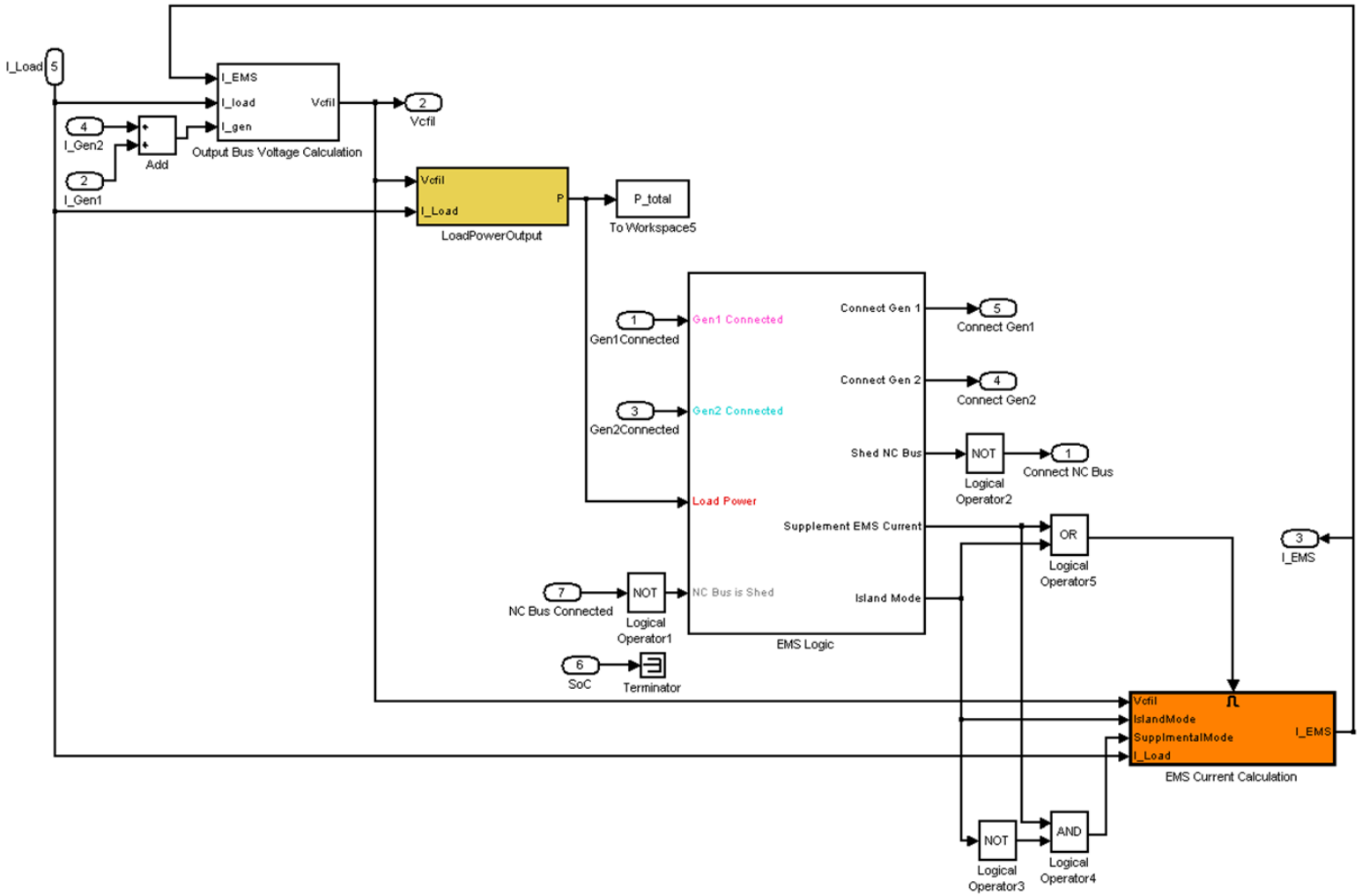

Figure 44. EMS.

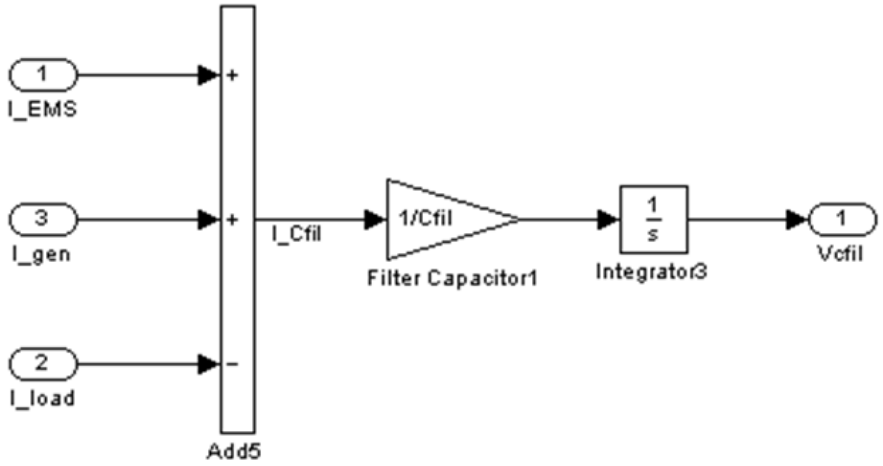

Figure 45. EMS -> Output bus calculation.

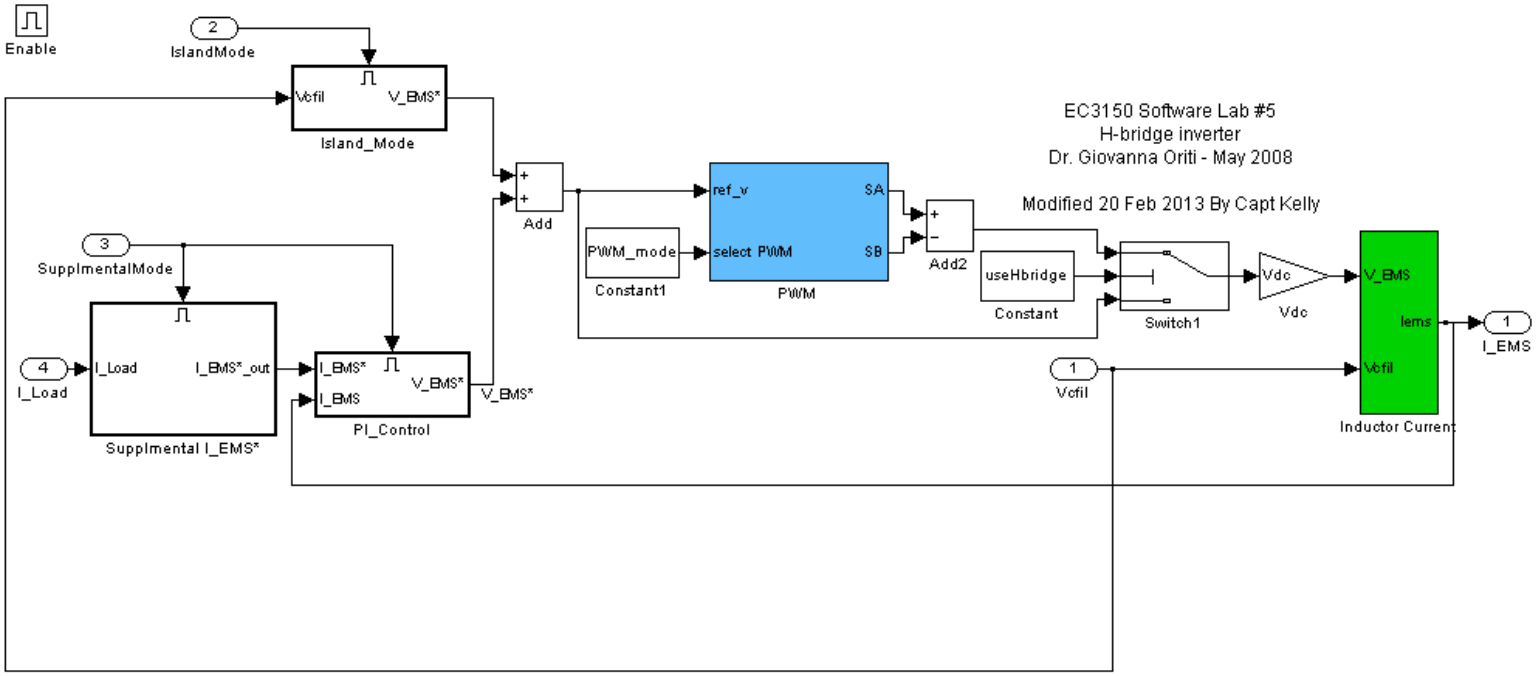

Figure 46. EMS -> EMS current calculation.

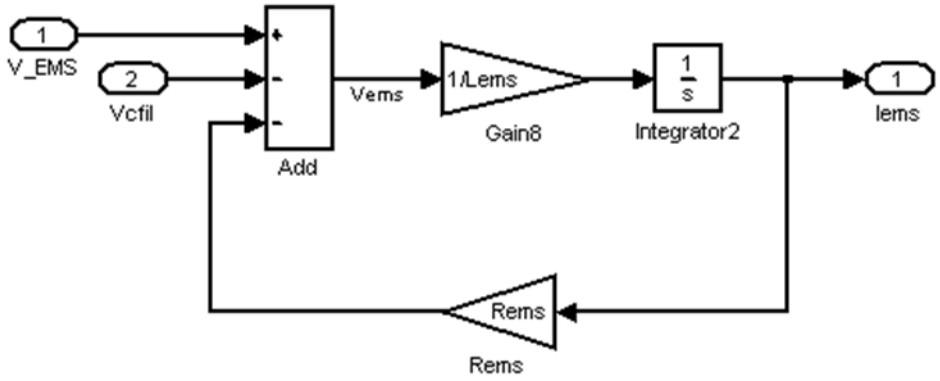

Figure 47. EMS -> EMS current calculation -> inductor current.

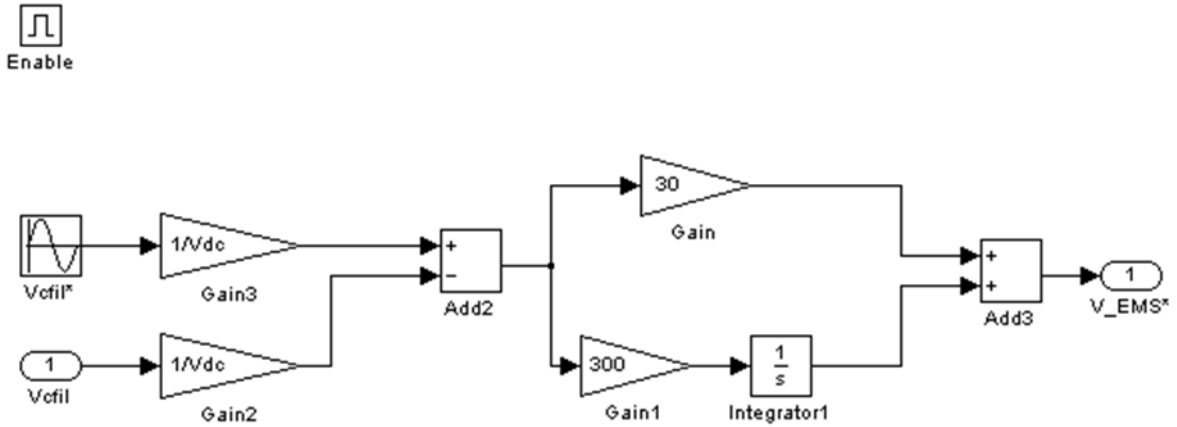

Figure 48. EMS -> EMS current calculation -> Island_mode.

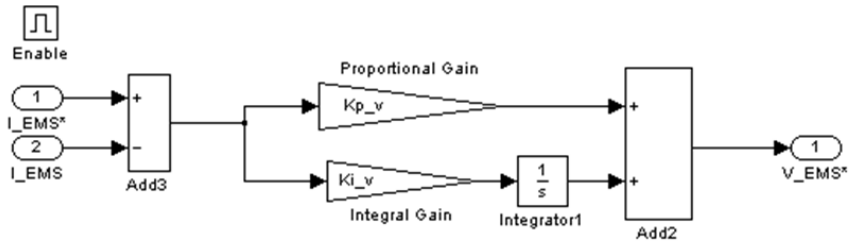

Figure 49. EMS -> EMS current calculation -> PI_control.

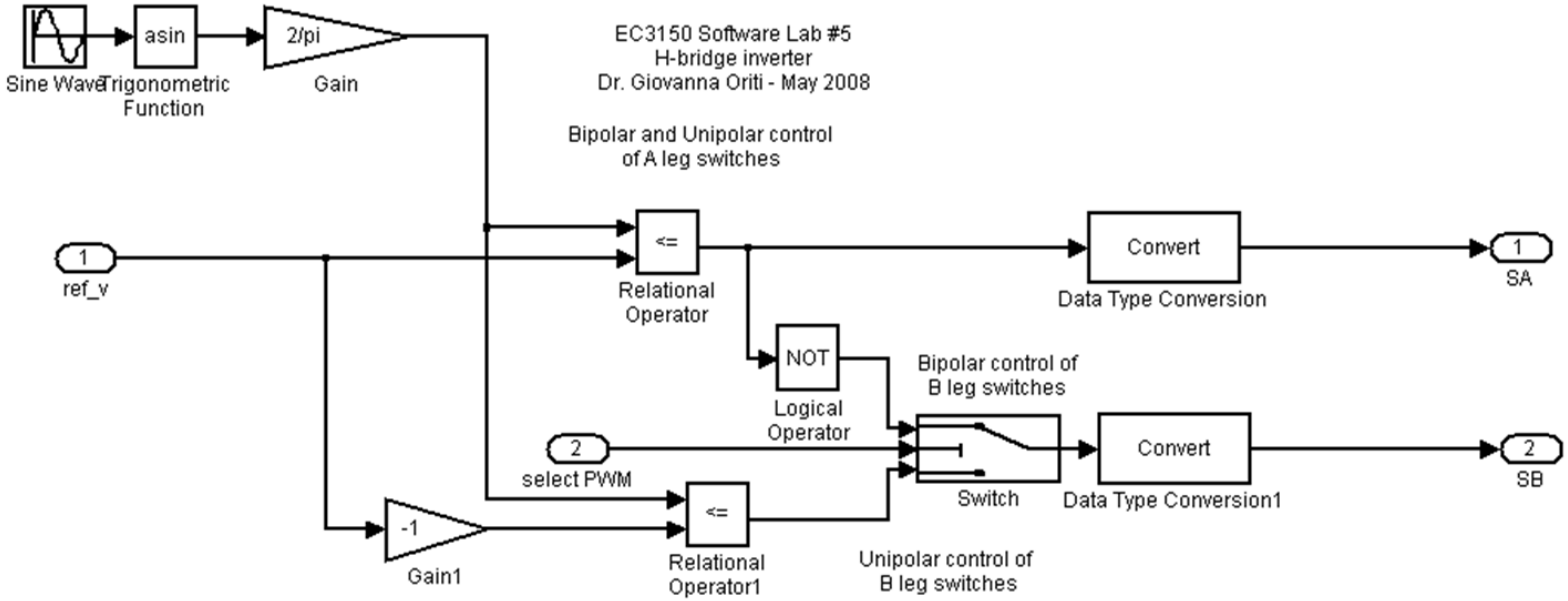

Figure 50. EMS -> EMS current calculation -> PWM.

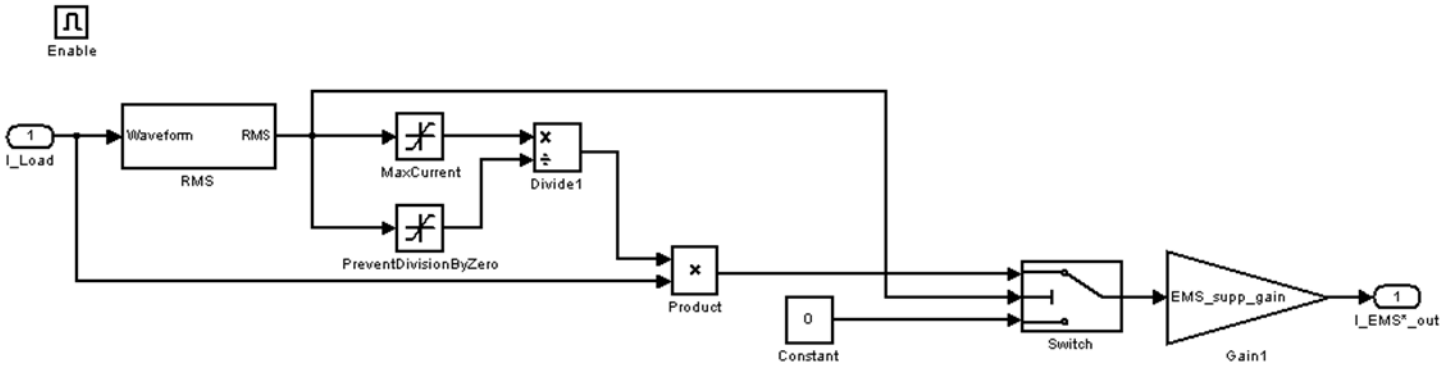

Figure 51. EMS -> EMS current calculation -> supplemental I_EMS*.

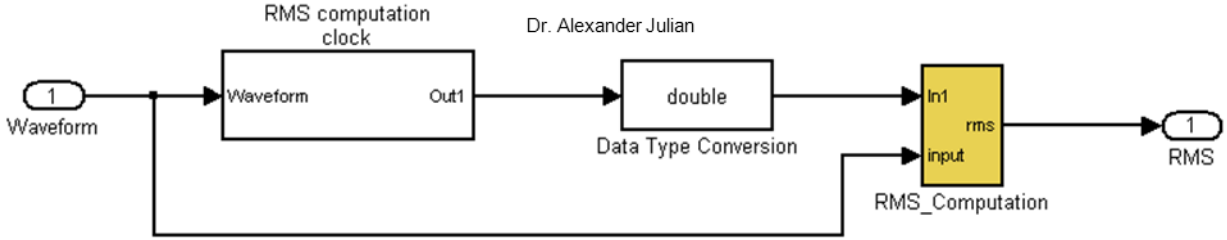

Figure 52. EMS -> EMS current calculation -> supplemental I_EMS* -> RMS.

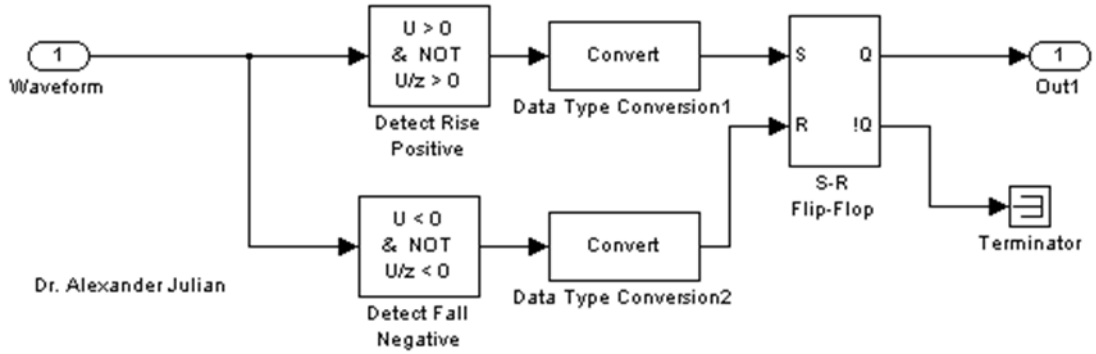

Figure 53. EMS -> EMS current calculation -> supplemental I_EMS* -> RMS -> RMS computation clock.

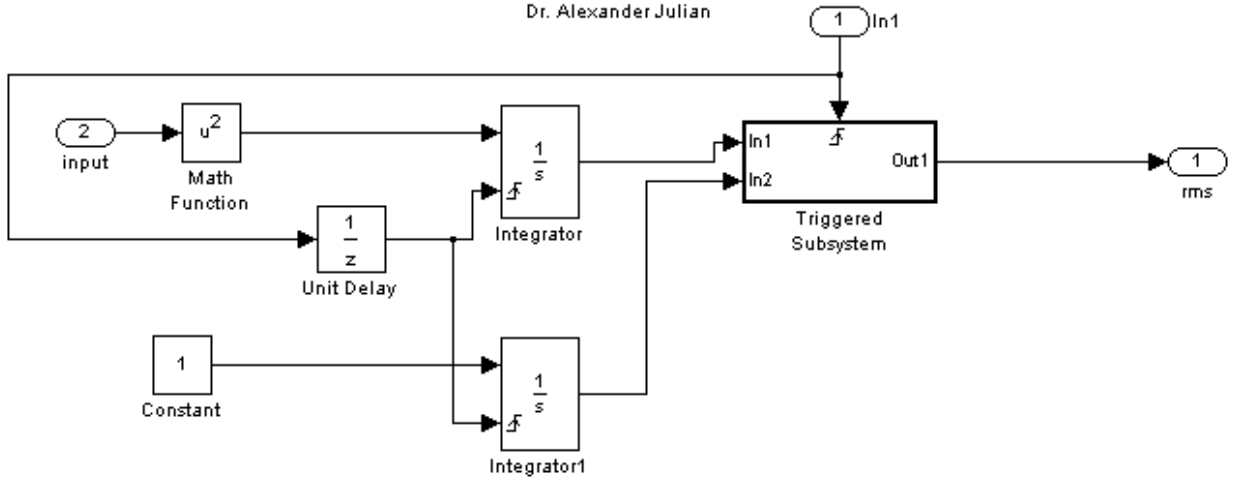

Figure 54. EMS -> EMS current calculation -> supplemental I_EMS* -> RMS -> RMS_computation.

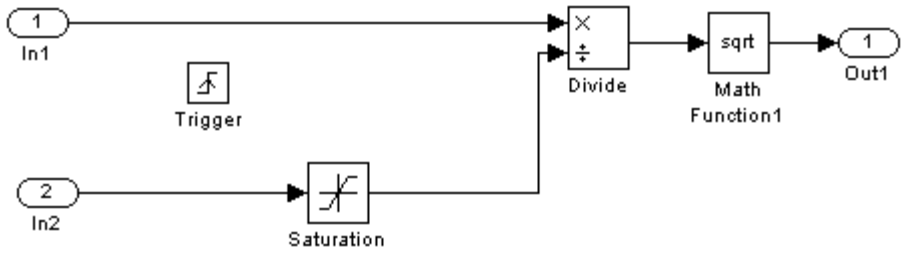

Figure 55. EMS -> EMS current calculation -> supplemental I_EMS* -> RMS -> RMS_computation -> triggered subsystem.

THIS PAGE INTENTIONALLY LEFT BLANK

LIST OF REFERENCES

[1] R. Tiron, "$400 per gallon gas to drive debate over cost of war in Afghanistan," *The Hill*, [Online]. Available: http://thehill.com/homenews/administration/63407–400gallon-gas-another-cost-of-war-in-afghanistan.

[2] B. Frazee, "Energy symposium looks at reducing the load in Marine Corps expeditionary operations," in U. S. Marine Corps Forces Reserve, February 2010, [Online]. Available: http://www.marforres.marines.mil/MFRNews/NewsArticleDisplay/tabid/7930/Article/81664/.

[3] E. Shields, B. Newell, "Current power and energy requirements of forward deployed USMC locations," Released January 2012.

[4] "Hybridization tradeoffs," Naval Sea Systems Command (NAVSEA) Warfare Centers Carderock, U. S. Navy, Bethesda, MD.

[5] J. Popović-Gerber, J.A. Oliver, N. Cordero, T. Harder, J.A. Cobos, M. Hayes, S.C. O'Mathuna, and E. Prem, "Power electronics enabling efficient energy usage: energy savings potential and technological challenges," in *IEEE Trans. Power Electron*., vol. 27, no. 5, pp. 2338–2353, May 2012.

[6] Boroyevich, I. Cvetkovi´c, D. Dong, R. Burgos, F. Wang, and F. Lee, "Future electronic power distribution systems—a contemplative view," in Proc. 12th International Conference on Optimization of Electrical and Electronic Equipment OPTIM '10, Brasov, Romania, pp. 1369–1380, 2010.

[7] S. Chakraborty, M. D. Weiss, M. G. Simões, "Distributed intelligent energy management system for a single-phase high-frequency AC microgrid," IEEE Trans. on Industrial Electronics, vol. 54, no.1, February 2007.

[8] E. Barklund, N. Pogaku, M. Prodanovic´, C. Hernandez-Aramburo, T. C. Green, "Energy management in autonomous microgrid using stability-constrained droop control of inverters," IEEE Trans. on Power Electronics, vol. 23, no. 5, September 2008.

[9] G. Oriti, A.L. Julian, N.J. Peck, "Power electronics enabled energy management systems," in Proceedings of IEEE Applied Power Electronics Conference, Long Beach, CA, March 2013.

[10] G. Byeon, T. Yoon, S. Oh, G. Jang, "Energy management strategy of the DC distribution system in buildings using the EV service model," IEEE Trans. on Power Electronics, vol. 28, no. 4, April 2013.

[11] "Guide to employing renewable energy and energy efficient technologies," Marine Corps Warfighting Laboratory, U.S. Marine Corps.

[12] "Technology comparison," Energy Storage Association. [Online]. Available: http://www.electricitystorage.org/technology/storage_technologies/technology_comparison.

[13] "Approximate diesel fuel consumption chart," [Online]. Available: http://www.dieselserviceandsupply.com/Diesel_Fuel_Consumption.aspx.

[14] "E2O update, 08 Nov 2011," USMC Expeditionary Power Systems, U.S. Marine Corps, Quantico, VA.

[15] J.B. Andriully et al., "Advanced power generation systems for the 21st century: market survey and recommendations for a design philosophy," Oak Ridge National Laboratory report ORNL/TM-1999/213, [Online]. Available: http://www.ornl.gov/~webworks/cpr/v823/rpt/104704.pdf

INITIAL DISTRIBUTION LIST

1. Defense Technical Information Center
   Ft. Belvoir, Virginia

2. Dudley Knox Library
   Naval Postgraduate School
   Monterey, California